

AD-777 841

A COMPUTER CODE FOR HIGH ALTITUDE EMP

Terry C. Chapman

Air Force Institute of Technology
Wright-Patterson Air Force Base, Ohio

January 1974

DISTRIBUTED BY:

NTIS

National Technical Information Service
U. S. DEPARTMENT OF COMMERCE
5285 Port Royal Road, Springfield Va. 22151

A COMPUTER CODE FOR
HIGH ALTITUDE EMP

THESIS

GNE/PH/74-1

Terry C. Chapman
Capt USAF



Approved for public release; distribution unlimited.

ib

A COMPUTER CODE FOR
HIGH ALTITUDE EMP

THESIS

Presented to the Faculty of the School of Engineering
of the Air Force Institute of Technology

Air University

in Partial Fulfillment of the
Requirements for the Degree of
Master of Science

by

Terry C. Chapman, B.S.
Capt USAF
Graduate Nuclear Engineering


January 1974

Approved for public release; distribution unlimited.

ic

UNCLASSIFIED

SECURITY CLASSIFICATION OF THIS PAGE (When Data Entered)

REPORT DOCUMENTATION PAGE		READ INSTRUCTIONS BEFORE COMPLETING FORM
1. REPORT NUMBER GNE/PH/74-1	2. GOVT ACCESSION NO.	3. RECIPIENT'S CATALOG NUMBER AD 777841
4. TITLE (and Subtitle) A COMPUTER CODE FOR HIGH ALTITUDE EMP		5. TYPE OF REPORT & PERIOD COVERED THESIS
		6. PERFORMING ORG. REPORT NUMBER
7. AUTHOR(s) Terry C. Chapman, Captain, USAF		8. CONTRACT OR GRANT NUMBER(s)
9. PERFORMING ORGANIZATION NAME AND ADDRESS AFIT/ENP Wright-Patterson AFB, OH 45433		10. PROGRAM ELEMENT, PROJECT, TASK AREA & WORK UNIT NUMBERS
11. CONTROLLING OFFICE NAME AND ADDRESS AFIT/ENP Wright-Patterson AFB, OH 45433		12. REPORT DATE January 1974
		13. NUMBER OF PAGES 82
14. MONITORING AGENCY NAME & ADDRESS (if different from Controlling Office) Air Force Weapons Laboratory/EL Kirtland AFB, New Mexico 87117		15. SECURITY CLASS. (of this report) UNCLASSIFIED
		15a. DECLASSIFICATION/DOWNGRADING SCHEDULE
16. DISTRIBUTION STATEMENT (of this Report) Approved for public release; distribution unlimited		
17. DISTRIBUTION STATEMENT (of the abstract entered in Block 20, if different from Report)		
18. SUPPLEMENTARY NOTES Approved for public release; IAW AFR 190-17. <div style="text-align: right;">  JERRY C. HIX, Captain, USAF Director of Information </div>		
19. KEY WORDS (Continue on reverse side if necessary and identify by block number) EMP High Altitude EMP EMP Computer Code <div style="text-align: center;"> Reproduced by NATIONAL TECHNICAL INFORMATION SERVICE U S Department of Commerce Springfield VA 22151 </div>		
20. ABSTRACT (Continue on reverse side if necessary and identify by block number) A relatively inexpensive computer code is developed to calculate the peak value of the electric field contained in an electromagnetic pulse generated by the gamma rays from a high altitude nuclear burst. The code is based on the Karzas and Latter theory for the production of Compton electrons and their interaction with the earth's magnetic field. The code can be used to calculate the peak value of the electric field at a target anywhere on or above ground level.		

DD FORM 1473 1 JAN 73 EDITION OF 1 NOV 65 IS OBSOLETE

UNCLASSIFIED

SECURITY CLASSIFICATION OF THIS PAGE (When Data Entered)

20. resulting from a nuclear burst above 60 km altitude with a gamma yield up to 60 tons. Either the direct or the ground reflected wave can be calculated. With special care, bursts up to 1 kt of gamma yield can be used.

ia

Preface

It is my pleasure to recognize several people who contributed in various ways to make this work possible.

I want to thank my advisor, Maj Carl T. Case. His patience and helpful suggestions were important factors to the successful conclusion of this work. In addition, I want to point out that the theoretical portion of this work is based largely on a series of lectures he gave while teaching the Electromagnetic Waves (EE 6.30) course during the summer quarter of 1973. His unusual ability to present difficult topics in a way that is easily understood by the student was the largest and most important contribution to the success of this work.

I want to thank Dr. Charles J. Bridgman for his suggestions and helpful comments made during the early stages of the work.

I want to thank Capt Frank N. Fredrickson and Lt John R. Lillis for taking the time to discuss various problems, ideas, and solutions with me.

Last, but not least, I want to gratefully acknowledge the large contribution of my wife, Karen. She offered moral support, punched computer cards, typed drafts, and in many other ways contributed to the successful conclusion of this work.

Terry C. Chapman

Contents

Preface	ii
List of Figures	iv
Abstract	v
I. Introduction	1
II. Theory	4
Overview	4
Electron Current and Densities	4
Gamma Transport	4
Electron Currents and Densities	6
Relativistic Electron Motion	9
Transformation to Spherical Coordinates	10
Electromagnetic Fields from High Altitude Currents	13
Maxwell's Equations	13
Transformation to Spherical Coordinates and Retarded Time	14
High Frequency Approximation	17
III. Code Description	20
General Approach	20
Inputs	24
Preliminary Calculations	25
Calculation of Compton Currents and Conductivity	25
Integration of Field Equations	27
Outputs	27
IV. Results of Input Parameter Variation	29
V. Discussion and Recommendations	40
Limitations	40
Uses	41
Recommendations	41
Bibliography	43
Appendix A: EMP Code User's Guide	44
Appendix B: EMP Code Flow Charts	48
Appendix C: EMP Code Listing	57
Vita	73

List of Figures

<u>Figure</u>		<u>Page</u>
1.	Geometry of the Burst	5
2.	Descriptive Flow Chart	21
3.	Target Geometry	23
4.	Output from a Typical Run	30
5.	Plot of $E(\tau)$ at Target from a Typical Run	31
6.	Variation in the X Direction	33
7.	Variation in the Y Direction	34
8.	Variation in the Z Direction	35
9.	Variation in Height of Burst	37
10.	Variation in Gamma Yield	39

A COMPUTER CODE FOR HIGH ALTITUDE EMP

I. Introduction

The effects of a nuclear environment on aerospace systems is an important factor in systems analysis. During the past few years several students have worked with Professor Bridgman at the Air Force Institute of Technology (AFIT) on a computer code to determine survivability of a system with known nuclear vulnerabilities from a variable nuclear threat. The AFIT survivability code capabilities include blast, thermal, x-ray, gamma ray, and neutron effects. The high altitude EMP code presented in this report is intended to be used in conjunction with the AFIT survivability code.

The EMP (electromagnetic pulse) from a nuclear weapon is usually considered to be a radiating electromagnetic wave of short duration containing many frequencies. However, the nuclear generated EMP was not studied seriously until a considerable time after the first nuclear explosion. At present there is a significant amount of work being done to model EMP generation and effects. For example the Air Force Weapons Laboratory (AFWL) and several civilian companies under contract to the USAF are working in the field.

There are several different types of EMP with distinctions made between the mechanisms which generate them. Kinsley (Ref 1) presents a comprehensive discussion of the various types of EMP. For example, a nuclear burst on the ground produces an EMP with different characteristics

than those from a high altitude burst. Also, nuclear burst products interacting directly with a system can produce an EMP within the system or even within the circuits of the system. This report considers only the EMP generated by high altitude burst gamma rays interacting with the atmosphere.

The high altitude EMP code developed in this report is based on the theory of Karzas and Latter (Ref 2). Briefly, the theory develops a model for the interaction of Compton electrons with the geomagnetic field. The Compton electrons are produced by prompt gamma radiation from the burst in a reasonably well defined region in the atmosphere. Several simplifications are made before arriving at the final equations.

Since several of the simplifications and assumptions used are implicit in the presentation of the theory, it is appropriate to list them here. Only one group of monoenergetic unscattered gamma rays are considered to produce Compton electrons. Each gamma which interacts is assumed to produce one and only one Compton electron initially traveling precisely in the radial direction. No angular distribution of Compton electrons is allowed. All Compton electrons are assumed to have the same energy. Curvature of the Earth's magnetic field is ignored. The electromagnetic fields are not self-consistent, that is, only the geomagnetic field is considered to affect the motion of the Compton electrons. Cascading of secondary electrons and recombination of ions is ignored. The low

frequency portion of the pulse is not considered. The Earth is assumed to be flat and the finite conductivity of ground is not considered. The burst is assumed to be far from the absorption region. Only gamma ray effects are considered.

Although the final model is somewhat restricted by these assumptions and simplifications, the end result is a relatively inexpensive computer code which gives a peak value of the electric field at any target point on or above the ground, which is an upper bound on the actual peak value.

Section II of this report develops the theory and derives the equations used in the code. Section III describes the calculational procedures used in the code. Section IV presents a sample of typical results and a study of input parameter variation. Section V is a discussion of the code's limitations and uses, with recommendations for possible improvements. Appendix A is a code user's guide. Appendix B is the detailed flow charts for the entire code. And finally Appendix C is a listing of the complete code.

II. Theory

Overview

The EMP problem is a problem in classic electromagnetic theory. A solution of Maxwell's equations is a solution of the problem. In this case it is necessary to model the current and charge densities generated by the gamma rays in the absorption region to obtain the sources and conductivity needed to solve Maxwell's equations.

Expressions for the current sources and conductivity are obtained in four steps. The transport of the gammas from the burst to the absorption region is used to obtain the number density of reacting gammas. This result is used with the models for the current and charge densities to obtain preliminary expressions. Then after considering the relativistic motion of the Compton electrons, the preliminary expressions are transformed to spherical coordinates.

After presenting Maxwell's equations in a convenient form, they are transformed to spherical coordinates and retarded time. A high frequency approximation is then made to arrive at the final equations.

Electron Current and Density

Gamma Transport. Consider the geometry shown in Fig. 1. The nuclear burst occurs at the origin at time, $t = 0$. The gamma rays move to point r' in time t' and at that point and time interact to create Compton electrons. It is assumed

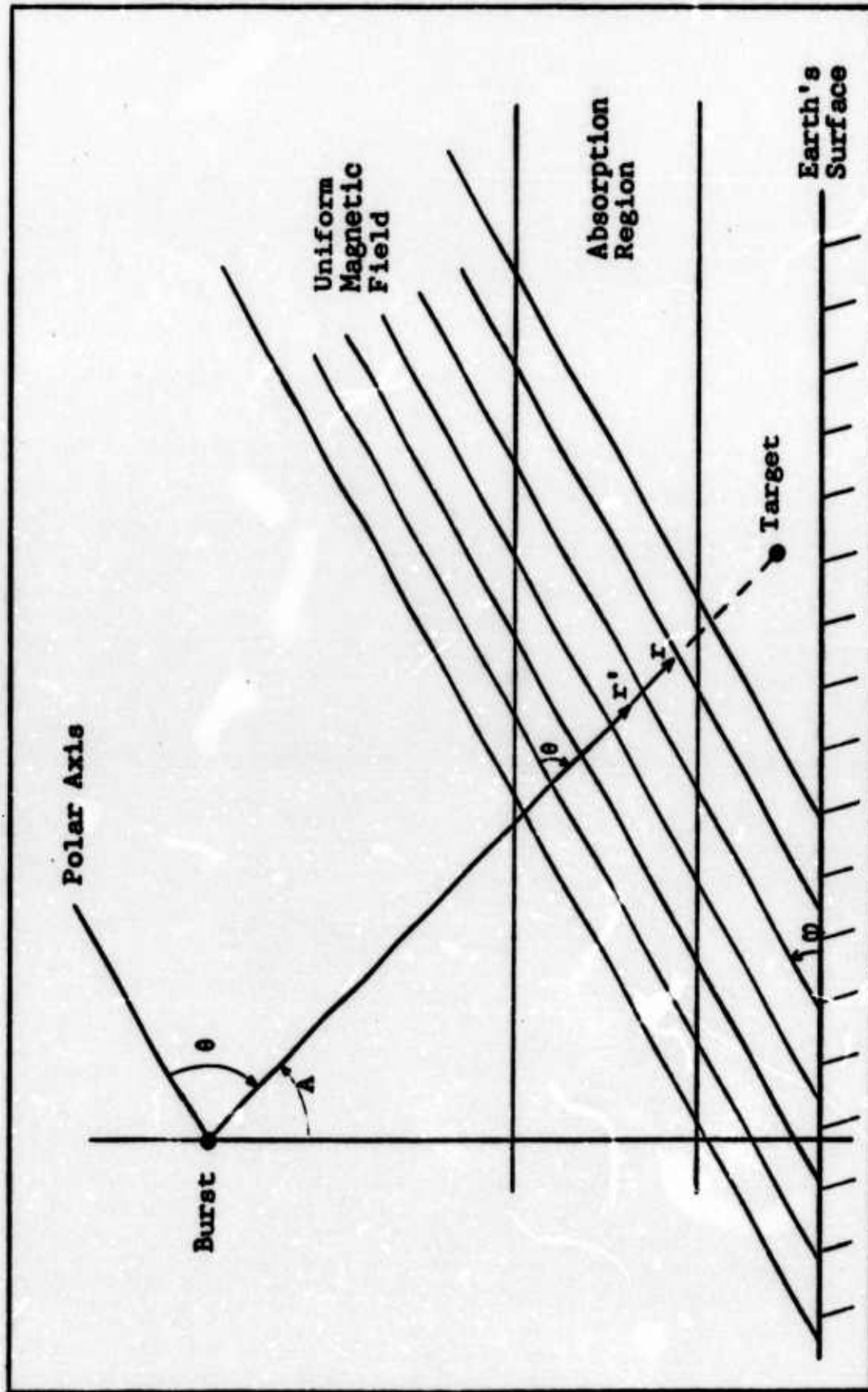


Fig. 1. Geometry of the Burst

that each gamma creates one and only one Compton electron traveling in the radial direction with the maximum Compton recoil energy.

The gamma ray emission rate can be taken as

$$\frac{dN(t)}{dt} = \frac{Y}{E} f(t) \quad (1)$$

where

$N(t)$ = number of gamma rays emitted

Y = gamma ray yield of burst

E = mean energy of the gamma rays

$f(t)$ = time dependence of the yield

and

$$\int_{-\infty}^{\infty} f(t) dt = 1 \quad (2)$$

The number density of gammas, $g(r)$, which interact at a point, r , can be taken as

$$g(r) = \frac{Y}{E} \frac{\exp \left\{ -\int_0^r \frac{dr'}{\lambda(r')} \right\}}{4\pi r^2 \lambda(r)} \quad (3)$$

where

λ = mean free path for production of Compton electrons.

Electron Currents and Densities. The rate of production of primary (Compton) electron density, n_{pri} , is

$$\frac{dn_{pri}}{dt} = g(r) f(t - r/c) \quad (4)$$

Following the Karzas-Latter approach (Ref 2) it is assumed that the electrons maintain their initial speed, V_0 , throughout their range, R , and then abruptly stop. Also, it is assumed that the secondary electrons are made at a uniform rate during the lifetime, R/V_0 , of the Compton electrons. Therefore, the rate of production of secondary electron density, n_{sec} , is

$$\frac{dn_{sec}}{dt} = \left\{ \frac{E_{pri}/33ev}{R/V_0} \right\} n_{pri} = \frac{qV_0}{R} n_{pri} \quad (5)$$

where

E_{pri} = the initial energy of the Compton electrons

R = the range of the Compton electrons in air

q = $E_{pri}/33ev$

$33ev$ = average ionization energy per molecule for
air

V_0 = the speed of the Compton electrons

R/V_0 = the lifetime of the Compton electrons

Now consider the current resulting from the Compton electrons. The differential current is the charge times the velocity times the differential density of electrons.

Hence

$$dJ^c = -e\vec{V}(t-t')g(r')f(t' - r'/c)dt' \quad (6)$$

where

$\vec{V}(t-t')$ = velocity of the Compton electrons at
time t which were created at time t' .

Putting (6) into integral form gives

$$\vec{j}^c = -e \int_{t-R/V_0}^t g(r') f(t' - r'/c) \vec{V}(t-t') dt' \quad (7)$$

Now let

$$\tau' = t - t' \quad (8a)$$

$$\tau = t - (r/c) \quad (8b)$$

$$X(\tau') = X(\tau) = r - r' \quad (8c)$$

Also note that

$$(r-r') \ll r \text{ or } r' \quad (9)$$

for distant explosions (see Fig. 1). So,

$$g(r) = g(r') \quad (10)$$

Using Eqs (8), (9), and (10) in Eq (7) gives

$$\vec{j}^c = -eg(r) \int_0^{R/V_0} \vec{V}(\tau') f\left(\tau - \tau' + \frac{X(\tau')}{c}\right) d\tau' \quad (11)$$

Using similar arguments,

$$n_{pri} = g(r) \int_0^{R/V_0} f\left(\tau - \tau' + \frac{X(\tau')}{c}\right) d\tau' \quad (12)$$

And putting Eq (12) into Eq (5) yields

$$n_{\text{sec}} = \frac{qV_0}{R} \int_{-\infty}^{\tau} n_{\text{pri}}(\tau') d\tau'$$

$$= g(\tau) \frac{qV_0}{R} \int_{-\infty}^{\tau} \left[\int_0^{R/V_0} f\left(\tau' - \tau'' + \frac{X(\tau'')}{c}\right) d\tau'' \right] d\tau' \quad (13)$$

Relativistic Electron Motion. Equations (11), (12), and (13) contain $r(\tau)$ and $X(\tau)$ which are not yet defined in an easily obtained form. The equation of motion for a Compton electron is

$$\frac{d}{d\tau} (m\gamma\vec{V}) = -e\vec{V}\times\vec{B}_0 \quad (14)$$

where

m = electron rest mass

$\gamma = [1 - (V/c)^2]^{-1/2}$

\vec{B}_0 = earth's magnetic field = $B_0 \hat{U}_z$

Again it is assumed that V_0 is constant throughout the electron's lifetime.

With $\omega = eB_0/m\gamma$ Eq (14) becomes

$$\frac{d}{d\tau} \vec{V}(\tau) = -\vec{V}(\tau) \times \hat{U}_z \omega \quad (15)$$

Breaking Eq (15) into its rectangular components

$$\frac{dV_x}{d\tau} = -\omega V_y \quad (16a)$$

$$\frac{dV_y}{d\tau} = \omega V_x \quad (16b)$$

$$\frac{dV_z}{d\tau} = 0 \quad (16c)$$

A solution for this set of equations is

$$V_x = V_{\perp} \cos \omega\tau \quad (17a)$$

$$V_y = V_{\perp} \sin \omega\tau \quad (17b)$$

$$V_z = V_{\parallel} \quad (17c)$$

where V_{\perp} is the initial velocity component perpendicular to \vec{B}_0 and V_{\parallel} is the initial velocity component parallel to \vec{B}_0 and both are constants with respect to τ .

Transformation to Spherical Coordinates. It is convenient to transform the above solution to a spherical coordinate system with its origin at the burst point. The transformation from rectangular to spherical coordinates is

$$V_r = V_x \sin \theta \cos \phi + V_y \sin \theta \sin \phi + V_z \cos \theta \quad (18a)$$

$$V_{\theta} = V_x \cos \theta \cos \phi + V_y \cos \theta \sin \phi - V_z \sin \theta \quad (18b)$$

$$V_{\phi} = -V_x \sin \phi + V_y \cos \phi \quad (18c)$$

Without loss of generality the coordinates can be chosen such that \vec{V} lies in the X-Y plane, hence $\theta = 90^\circ$, and the transformation becomes

$$V_r = V_x \sin \theta + V_z \cos \theta \quad (19a)$$

$$V_\theta = V_x \cos \theta - V_z \sin \theta \quad (19b)$$

$$V_\phi = V_y \quad (19c)$$

Note that

$$V_\perp = V_0 \sin \theta \quad (20a)$$

$$V_{||} = V_0 \cos \theta \quad (20b)$$

Putting Eqs (17) and (20) into Eq (19) gives

$$V_r = V_0 [\sin^2 \theta \cos \omega \tau + \cos^2 \theta] \quad (21a)$$

$$V_\theta = V_0 [\cos \theta \sin \theta \cos \omega \tau - \sin \theta \cos \theta] \quad (21b)$$

$$V_\phi = V_0 [\sin \theta \sin \omega \tau] \quad (21c)$$

Now $X(\tau)$ can be written as

$$X(\tau) = \int_0^\tau V_r d\tau = V_0 \left[\sin^2 \theta \frac{\sin \omega \tau}{\omega} + \tau \cos^2 \theta \right] \quad (22)$$

Equations (21) and (22) substituted into Eq (11) give

$$J_r^c = -eg(r)V_0 \int_0^{R/V_0} f(T) [\cos^2 \theta + \sin^2 \theta \cos \omega \tau'] d\tau' \quad (23)$$

$$J_\theta^c = -eg(r)V_0 \int_0^{R/V_0} f(T) [\sin \theta \cos \theta (\cos \omega \tau' - 1)] d\tau' \quad (24)$$

$$J_\phi^c = -eg(r)V_0 \int_0^{R/V_0} f(T) [\sin \theta \sin \omega \tau'] d\tau' \quad (25)$$

where

$$T = \tau - (1 - \beta \cos^2 \theta) \tau' + \beta \sin^2 \theta \frac{\sin \omega \tau'}{\omega} \quad (26a)$$

with

$$\beta = v_0/c \quad (26b)$$

Equations (23), (24), (25), and (26) provide the Compton currents within the absorption region in a form which can be used in the final field equations. In addition to the Compton currents, an expression for the conductivity within the absorption region is needed.

Equations (21) and (22) substituted into Eq (13) give

$$n_{\text{sec}}(\tau) = \frac{qv_0}{R} g(\tau) \int_{-\infty}^{\tau} \left[\int_0^{R/v_0} f(T') dT' \right] d\tau' \quad (27)$$

where

$$T' = \tau' - (1 - \beta \cos^2 \theta) \tau'' + \beta \sin^2 \theta \frac{\sin \omega \tau''}{\omega} \quad (28)$$

Consider the equation of motion for secondary electrons. Neglecting the $\vec{v} \times \vec{B}_0$ term, which is small compared to the other terms (Ref 2) it is

$$m \frac{d\vec{v}}{dt} = -e\vec{E} - m\vec{v}v_c \quad (29)$$

where

v_c = electron collision frequency.

These secondary electrons have velocities in the thermal region and are assumed to reach their maximum velocity instantly. In this case, Eq (29) becomes

$$\vec{V} = \frac{-e}{mv_c} \vec{E} \quad (30)$$

The current source from the secondary electrons is

$$\vec{j}^{sec} = -e\vec{V}(\tau)n_{sec}(\tau) = \frac{n_{sec}(\tau)}{mv_c} e^2 \vec{E} \quad (31)$$

or in terms of conductivity

$$\vec{j}^{sec} = \sigma(\tau)\vec{E} \quad (32)$$

where

$$\sigma(\tau) = \frac{n_{sec}(\tau)}{mv_c} e^2 \quad (33)$$

Equations (32) and (33) provide the needed expressions for the conductivity.

Electromagnetic Fields from High Altitude Currents

Maxwell's Equations. Now that the Compton currents and the conductivity due to secondary electrons have been obtained, consider the field equations.

Maxwell's equations are

$$\vec{\nabla} \times \vec{E} = - \frac{\partial \vec{B}}{\partial t} \quad (34a)$$

$$\vec{\nabla} \times \vec{B} = \mu_0 \vec{J} + \frac{1}{c^2} \frac{\partial \vec{E}}{\partial t} \quad (34b)$$

$$\vec{\nabla} \cdot \vec{E} = \frac{q_v}{\epsilon_0} \quad (34c)$$

$$\vec{\nabla} \cdot \vec{B} = 0 \quad (34d)$$

where

\vec{J} = total current density

q_v = total charge density

Continuity of charge requires

$$\frac{\partial q_v}{\partial t} + \vec{\nabla} \cdot \vec{J} = 0 \quad (35)$$

It is convenient to combine the above equations into equations containing only \vec{E} in one and only \vec{B} in the other. Doing so gives

$$\left(\nabla^2 - \frac{1}{c^2} \frac{\partial^2}{\partial t^2} \right) \vec{E} = \mu_0 \frac{\partial \vec{J}}{\partial t} + \frac{1}{\epsilon_0} \vec{\nabla} q_v \quad (36)$$

$$\left(\nabla^2 - \frac{1}{c^2} \frac{\partial^2}{\partial t^2} \right) \vec{B} = -\mu_0 \vec{\nabla} \times \vec{J} \quad (37)$$

Transformation to Spherical Coordinates and Retarded Time. Equations (36) and (37) will now be transformed to spherical coordinates and retarded time. Consider the transformation

$$\tau = t - r/c \quad (38a)$$

$$r' = r \quad (38b)$$

$$\theta' = \theta \quad (38c)$$

$$\phi' = \phi \quad (38d)$$

This is a spherical coordinate system where time is measured at each radial point in terms of the arrival of the bomb gamma rays at that point.

Using Eq (38) it is easily shown that

$$\frac{\partial}{\partial t} = \frac{\partial}{\partial \tau} \quad (39)$$

$$\frac{\partial}{\partial r} = \frac{\partial}{\partial r'} - \frac{1}{c} \frac{\partial}{\partial \tau} \quad (40)$$

$$\frac{\partial}{\partial \theta} = \frac{\partial}{\partial \theta'} \quad (41)$$

$$\frac{\partial}{\partial \phi} = \frac{\partial}{\partial \phi'} \quad (42)$$

Thus the operator

$$\frac{\partial}{\partial t}$$

transforms to

$$\frac{\partial}{\partial \tau}$$

and the operator

$$\vec{\nabla}$$

transforms to

$$\vec{\nabla} - \hat{U}_r \frac{1}{c} \frac{\partial}{\partial \tau}$$

Similarly, the operator

$$\nabla^2 - \frac{1}{c^2} \frac{\partial^2}{\partial \tau^2}$$

transforms to

$$\nabla^2 - \frac{2}{c} \frac{\partial}{\partial \tau} \frac{1}{r} \frac{\partial}{\partial r} r$$

Equation (36) now becomes

$$\left[\nabla^2 - \frac{2}{c} \frac{1}{r} \frac{\partial}{\partial \tau} \frac{\partial}{\partial r} r \right] \vec{E} = \mu_0 \frac{\partial \vec{J}}{\partial \tau} + \frac{1}{\epsilon_0} \vec{\nabla} q_v - \hat{U}_r \frac{1}{c} \frac{\partial q_v}{\partial \tau} \quad (43)$$

and Eq (35) becomes

$$\frac{\partial q_v}{\partial \tau} = -\vec{\nabla} \cdot \vec{J} + \hat{U}_r \frac{1}{c} \frac{\partial}{\partial \tau} \cdot \vec{J} = -\vec{\nabla} \cdot \vec{J} + \frac{1}{c} \frac{\partial J_r}{\partial \tau} \quad (44)$$

Using Eq (44) in Eq (43) and rearranging gives

$$\begin{aligned} & -\nabla^2 \vec{E} + \hat{U}_r \frac{1}{c \epsilon_0} \vec{\nabla} \cdot \vec{J} + \frac{1}{\epsilon_0} \vec{\nabla} q_v \\ & + \frac{\partial}{\partial \tau} \left[\frac{2}{c} \frac{1}{r} \frac{\partial}{\partial \tau} (r \vec{E}) + \mu_0 (\vec{J} - \hat{U}_r J_r) \right] = 0 \end{aligned} \quad (45)$$

Similarly, Eq (37) becomes

$$\begin{aligned}
 & -\nabla^2 \vec{B} + \mu_0 \nabla \times \vec{J} + \frac{\partial}{\partial \tau} \left[\frac{2}{rc} \frac{\partial}{\partial r} (r \vec{B}) \right] \\
 & + \frac{\partial}{\partial \tau} \left[\frac{\mu_0}{c} (\hat{U}_\phi J_\phi - \hat{U}_\theta J_\theta) \right] = 0 \quad (46)
 \end{aligned}$$

High Frequency Approximation. Again, following the Karzas-Latter model, note that the variation of currents with distance is slow compared to variations with time and that the fields resulting from the transverse currents are rapidly varying in character, as are the currents themselves. Therefore, only the $\partial/\partial\tau$ terms are kept in the transverse field equations. Since the radial components do not propagate outside of the absorption region, they are not considered further in this report.

The transverse equations become

$$\frac{\partial}{\partial \tau} \left[\frac{2}{c} \frac{1}{r} \frac{\partial}{\partial r} (r E_\theta) + \mu_0 J_\theta \right] = 0 \quad (47)$$

$$\frac{\partial}{\partial \tau} \left[\frac{2}{c} \frac{1}{r} \frac{\partial}{\partial r} (r E_\phi) + \mu_0 J_\phi \right] = 0 \quad (48)$$

$$\frac{\partial}{\partial \tau} \left[\frac{2}{c} \frac{1}{r} \frac{\partial}{\partial r} (r B_\theta) - \frac{\mu_0}{c} J_\phi \right] = 0 \quad (49)$$

$$\frac{\partial}{\partial \tau} \left[\frac{2}{c} \frac{1}{r} \frac{\partial}{\partial r} (r B_\phi) + \frac{\mu_0}{c} J_\theta \right] = 0 \quad (50)$$

These equations are called the Karzas-Latter high frequency approximation for the EMP fields, and they are useful in the range $0 < \tau < 100$ shakes.

Integration with respect to time yields

$$\frac{2}{c} \frac{1}{r} \frac{\partial}{\partial r} (rE_{\theta}) + \mu_0 J_{\theta} = 0 \quad (51)$$

$$\frac{2}{c} \frac{1}{r} \frac{\partial}{\partial r} (rE_{\phi}) + \mu_0 J_{\phi} = 0$$

$$\frac{2}{c} \frac{1}{r} \frac{\partial}{\partial r} (rB_{\theta}) - \frac{\mu_0}{c} J_{\phi} = 0 \quad (53)$$

$$\frac{2}{c} \frac{1}{r} \frac{\partial}{\partial r} (rB_{\phi}) + \frac{\mu_0}{c} J_{\theta} = 0 \quad (54)$$

Recall that the total current density is

$$\vec{j} = \vec{j}^{\text{pri}} + \vec{j}^{\text{sec}} = \vec{j}^{\text{c}} + \sigma(\tau)\vec{E} \quad (55)$$

so Eqs (51) and (52) become

$$\frac{2}{c} \frac{1}{r} \frac{\partial}{\partial r} (rE_{\theta}) + \mu_0 J_{\theta}^{\text{c}} + \mu_0 \sigma(\tau)E_{\theta} = 0 \quad (56)$$

$$\frac{2}{c} \frac{1}{r} \frac{\partial}{\partial r} (rE_{\phi}) + \mu_0 J_{\phi}^{\text{c}} + \mu_0 \sigma(\tau)E_{\phi} = 0 \quad (57)$$

With the aid of a computer, it is now possible to obtain numerical solutions for the above equations which will yield a slightly high estimate of the peak value of the EMP pulse resulting from a high altitude burst.

Below the absorption region the Compton currents and the conductivity are zero. In this case, Eqs (56) and (57) have the following solutions:

$$E_0 = C_1/r \quad (58)$$

$$E_\phi = C_2/r \quad (59)$$

where C_1 and C_2 are determined by the values of E_0 , E_ϕ , and r at the bottom of the absorption region.

III. Code Description

General Approach

Equations (56), (57), (58), and (59) were chosen as the simplest ones to solve numerically. Of course, Eqs (24), (25), (27), and (33) are used to obtain the Compton currents and conductivity needed to solve Eqs (56) and (57).

The B - field equations are not solved since

$$E = cB \quad (60)$$

can be used to obtain B once E is found. This relationship is based on the assumption that the EMP pulse is a spherical wave propagating in free space, below the absorption region.

The function used for the time dependence of the weapon yield is the one recommended by Pomranning (Ref 3).

$$f(\tau) = (1/N) \frac{(\alpha+\beta) \exp(\tau-\tau_0)}{\beta + \alpha \exp[(\alpha+\beta)(\tau-\tau_0)]} \quad (61)$$

where N is chosen such that

$$\int_0^{\infty} f(\tau) d\tau = 1 \quad (62)$$

and $\alpha > \beta$.

This function rises like $e^{\alpha\tau}$ for small τ , falls like $e^{-\beta\tau}$ for large τ , and has a single maximum at τ_0 .

Figure 2 presents a flow chart which is descriptive of the approach taken solving the equations. The top of the absorption region is assumed to be at 50 km altitude and the bottom of the absorption region is assumed to be

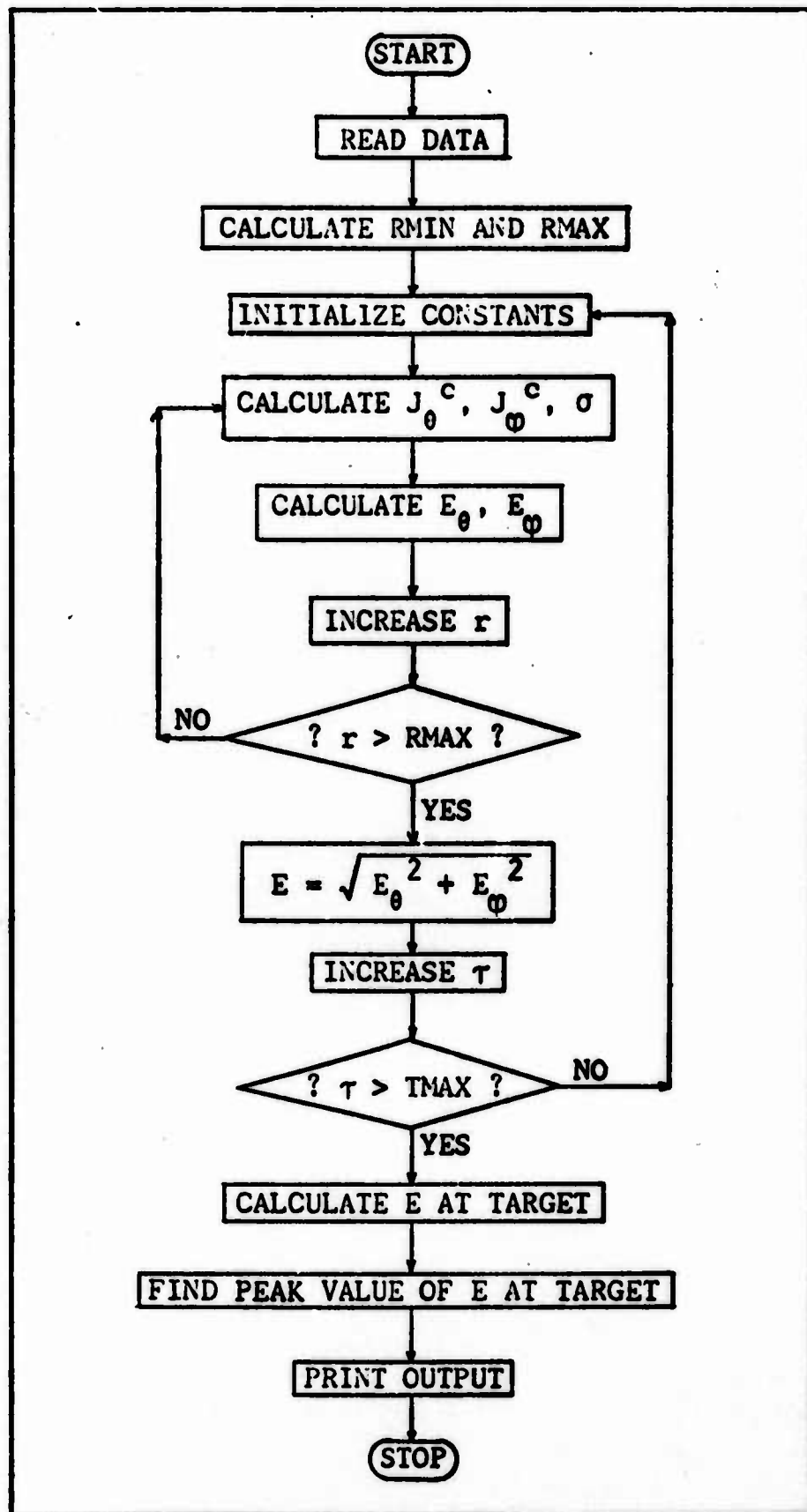


Fig. 2. Descriptive Flow Chart

at 20 km altitude. Calculations by Latter and LeLevier (Ref 4) indicate that 20 km to 50 km is the altitude where most of the prompt gamma ray energy is deposited.

Figure 3 depicts the target geometry. The value for RMIN is determined by the intersection of the line of sight with the 50 km altitude. The value for RMAX is determined by the intersection of the line of sight with the 20 km altitude. If the target is in the absorption region the target altitude determines RMAX for the direct wave calculation. These two values of r are the limits on the mesh in the r direction. The line of sight is divided into the desired number of steps along r for the integration on r in the absorption region.

The retarded time direction of the mesh is divided into 0.1 shake steps up to 10 shakes and then 1.0 shake steps on up to 100 shakes. Calculation can be stopped at any desired TMAX from 10 to 100 shakes, which is the upper limit of the usefulness of the high frequency approximation.

If the ground reflected wave is to be calculated, the mirror image of the target, below ground, is used to find the line of sight from the burst to the target. (Refer to Fig. 3.)

At $r = RMIN$ all of the fields are assumed to be zero. For each τ , equations (57) and (58) are integrated over r from RMIN to RMAX and the value of E at the bottom of the absorption region is stored. At each step in r, equations (24), (25), and (27) are numerically integrated. Then

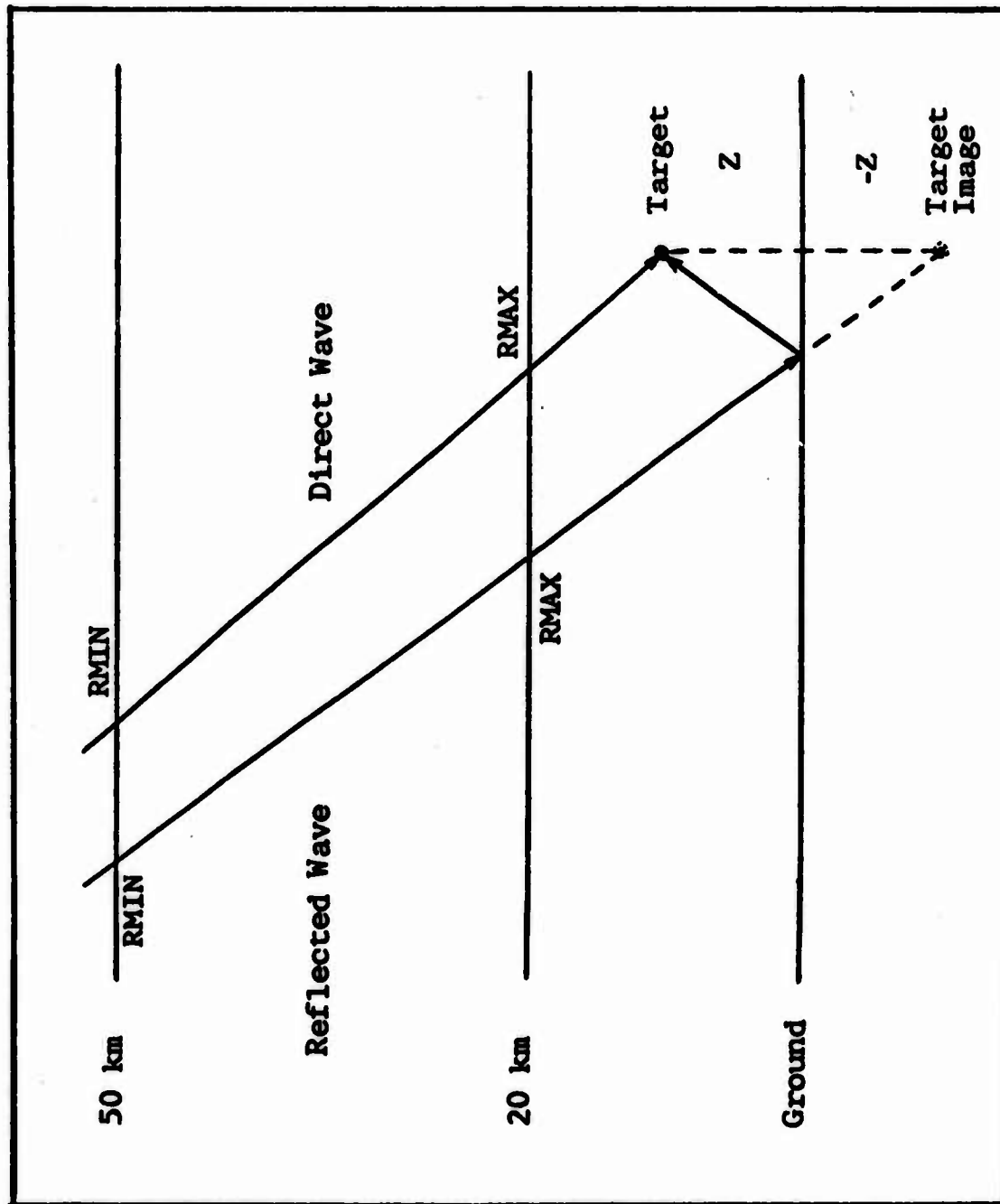


Fig. 3. Target Geometry

equations (58) and (59) are combined into

$$E = \frac{(R_{MAX})(E_{R_{MAX}})}{r_{target}} \quad (63)$$

to find E at the target.

The E array is then searched to find the peak value before printing out the results.

Inputs

The code uses a right handed Cartesian coordinate system with the ground in the X-Y plane, the \vec{B}_0 vector in the Y-Z plane, and \hat{j} pointing towards the equator. For example, in the northern hemisphere, \hat{i} is magnetic west, \hat{j} is magnetic south, and \hat{k} is altitude. The origin of the coordinate system is always at ground zero, directly below the burst. Note that this coordinate system is not the same as the Cartesian systems used earlier.

Referring to the above coordinate system the target coordinates, (X,Y,Z), are read in using units of meters. If the reflected wave is to be calculated the altitude is read in as a negative number, (X,Y,-Z).

The height of the burst is read in using units of kilometers. The gamma yield of the burst is read in using units of kilotons.

The magnitude of the Earth's magnetic field is read in using units of webers per square meter. The dip angle (ϕ in Fig. 1) of the magnetic field is read in using units of degrees.

NDELR, the desired number of steps to be used in the integration over r in the absorption region, is read in as any integer in the closed interval [50, 500].

TMAX, the retarded time where calculations are to be stopped, is read in, using units of shukes, as any integer in the closed interval [10, 100].

Preliminary Calculations

Before starting the numerical integrations, the code performs several preliminary calculations. The input data is converted to MKS units. The reflected wave is used whenever Z is greater than 49 km or less than 0. The target coordinates are transformed to a spherical coordinate system with the burst at the origin and the polar axis parallel to \vec{B}_0 . The line of sight intersections with the absorption region are determined. And finally, the constant angles required by the code, θ and A , (see Fig. 1) are calculated.

Calculation of Compton Currents and Conductivity

The two Compton currents, J_θ^C and J_ϕ^C are calculated at each r , τ mesh point by numerically integrating equations (24) and (25). The step size used is 0.1 times the Compton lifetime, R/V_0 . The integration itself is done using the 4th order Runge-Kutta method (Ref 5). It should be noted that both the mean free path for Compton interaction and the Compton lifetime are exponentially scaled from sea

level values using a 7 km scale height. However, the Compton lifetime is not allowed to be greater than 100 shakes, since this is the maximum time of interest.

Monoenergetic gammas of energy 1.5 Mev are assumed. The most energetic Compton electrons resulting from 1.5 Mev gammas have a speed of $2.88 (10)^8$ m/sec. Therefore $V_0 = 2.88 (10)^8$ m/sec.

Since the integration on τ'' in equation (27) is also over the Compton lifetime, this integration is carried out simultaneously with the Compton current integrations. Again, the 4th order Runge-Kutta method is used. It is broken into two parts, one for $-\infty < \tau' < 0$ and the other for $0 < \tau' < \tau$. In this case, $-\infty$ is defined to be the time when the first gamma ray reached the top of the absorption region, since no secondaries can be produced before that time.

The integration on τ' in equations (27) is also broken into two parts, one for $-\infty < \tau' < 0$ and the other for $0 < \tau' < \tau$. In the first case, integration is started at $\tau' = 0$ and proceeds to $\tau' = -(r-RMIN)/V_0$ in steps of $\Delta\tau' = -\Delta r/V_0$. In the second case, integration is started at $\tau' = 0$ and proceeds to $\tau' = \tau$ in steps of $\Delta\tau' = \Delta r$. In both cases, simple step integration is used. That is

$$\int f(\tau') d\tau' = \sum_{\text{all } i} (\Delta\tau'_i) [f(\tau'_i)] \quad (64)$$

The integration over τ' is carried out parallel to the integration of (56) and (57) over r (using space as a pseudo retarded time) and simultaneously with the increase in τ as the space integrations are repeated for each new τ .

This rather involved approach to solving equation (27) is necessary to save running time. A direct approach, with separate integrations, would at least triple or quadruple the total running time required for execution of the code.

Integration of the Field Equations

For each τ , equations (56) and (57) are integrated from $r = RMIN$ to $r = RMAX$ in steps of $\Delta r = (RMAX-RMIN)/NDEL R$ using the 4th order Runge-Kutta method. Then the magnitude of E is found from the two components and the result is stored in the E array. τ is increased by $\Delta \tau$ and the whole process is repeated until τ reaches $TMAX$.

On completion of the iterations, each member of the E array is multiplied by $RMAX/r_{target}$ (equation 62). Then the E array is searched to find the peak value.

Outputs

There are several output options available in the code. The basic output is:

1. Gamma yield and altitude of burst.
2. Target coordinates from ground zero.
3. Distance from burst to target.
4. A message indicating whether the direct or the reflected wave is being calculated.

5. The time period covered by the calculation.
6. The time when the peak value occurred.
7. The peak value of E at the target.
8. The τ and E arrays.

In addition, a linear and a log-log plot of $E(\tau)$ can be obtained. Also, a listing of the values of E at the bottom of the absorption region for each τ can be obtained. Either or both of these two options can be added to the basic output.

IV. Results and Input Parameter Variation

The output from a typical run is shown in Fig. 4.
The $E(\tau)$ calculated during the run is shown in Fig. 5.

The input data for this run was:

X	= 0 meters	(65a)
Y	= 0 meters	(65b)
Z	= 0 meters	(65c)
HOB	= 100 km	(65d)
Y_γ	= .001 kt	(65e)
B_0	= $2(10)^{-5}$ wb/m ²	(65f)
Dip Angle	= 20°	(65g)
NDEL R	= 50	(65h)
TMAX	= 20 shakes	(65i)

The CDC 6600 Computer required 191 sec and 33000_g words of central memory to execute this run.

The peak value of E, 6400 V/m, obtained in this run compares favorably with Karzas-Latter's order of magnitude estimate of 10^4 V/m (Ref 2) from similar input data.

In order to gain a better knowledge of the operating capabilities of the code, the effect of varying input parameters one at a time was studied. The basic set of parameters used was:

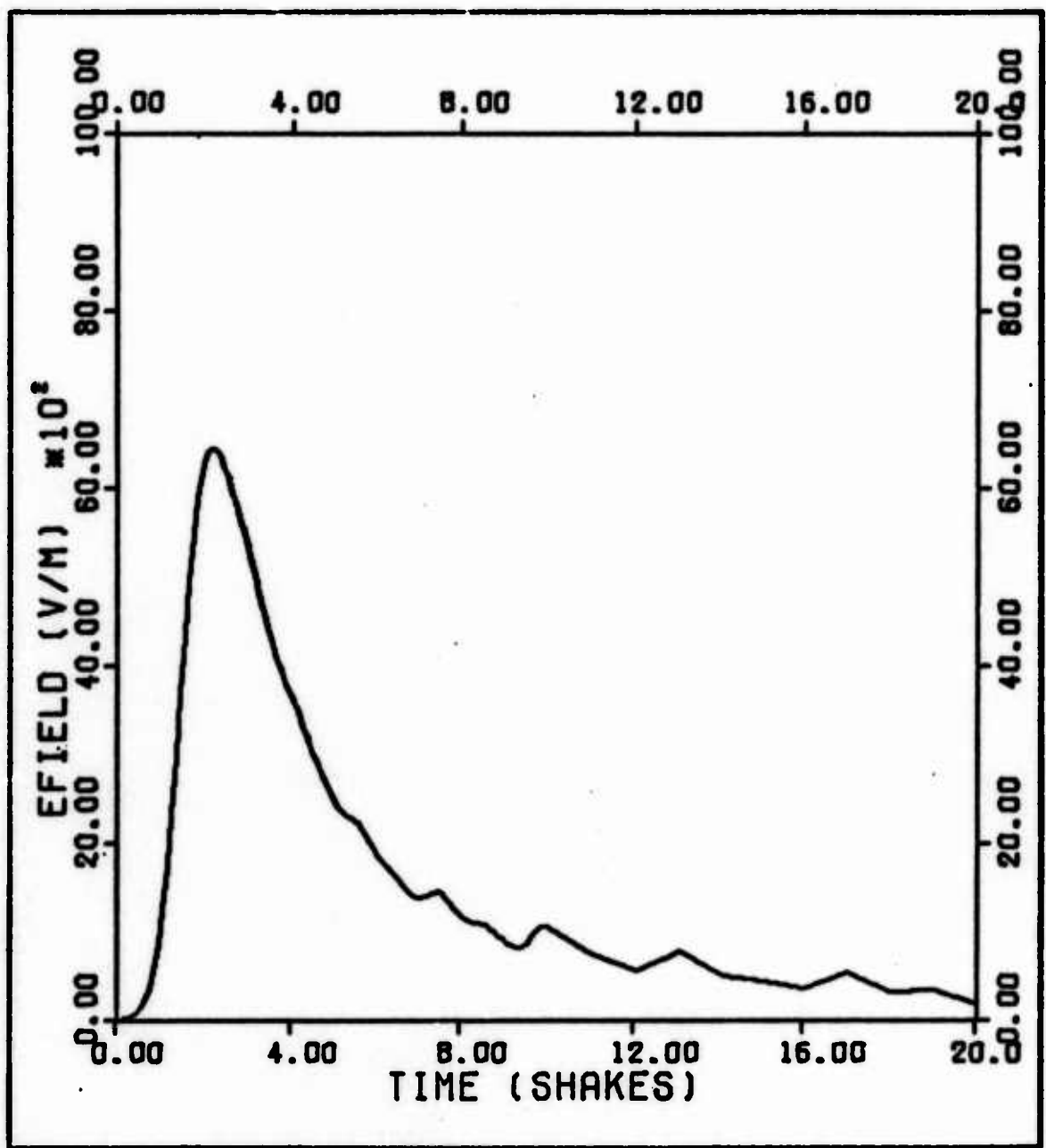


Fig. 5. Plot of E(τ) at target from a typical run

$$X = 0 \text{ meters} \quad (66a)$$

$$Y = 0 \text{ meters} \quad (66b)$$

$$Z = 0 \text{ meters} \quad (66c)$$

$$\text{HOB} = 100 \text{ km} \quad (66d)$$

$$Y_{\gamma} = .001 \text{ kt} \quad (66e)$$

Each of the above parameters was systematically varied while holding the others constant. The other inputs were held constant at the values shown in equations (65).

The results of the variation in X are shown in Fig. 6. Since the X axis is perpendicular to the magnetic field the symmetry about X = 0 is expected. The decrease in peak value of E for increasing distance from ground zero is due to the increasing distance from the burst.

The results of the variation in Y are shown in Fig. 7. Here the peak values of E depend on the angle between \vec{r} and \vec{B}_0 , θ . When $\theta = 180^\circ$ ($A = -70^\circ$ and $Y = -275 \text{ km}$) the peak E drops to zero. The maximum peak E is skewed toward $A = 20^\circ$ ($\theta = 90^\circ$ and $Y = 36 \text{ km}$). The maximum is not exactly at $A = 20^\circ$ because of the increased distance from the burst. These characteristics are expected since an electron moving perpendicular to the magnetic field would feel the strongest acceleration from it while an electron moving parallel to the magnetic field would feel no acceleration at all.

The results of variation in Z are shown in Fig. 8. In this case, both the direct and the reflected waves were calculated at each point below the top of the absorption

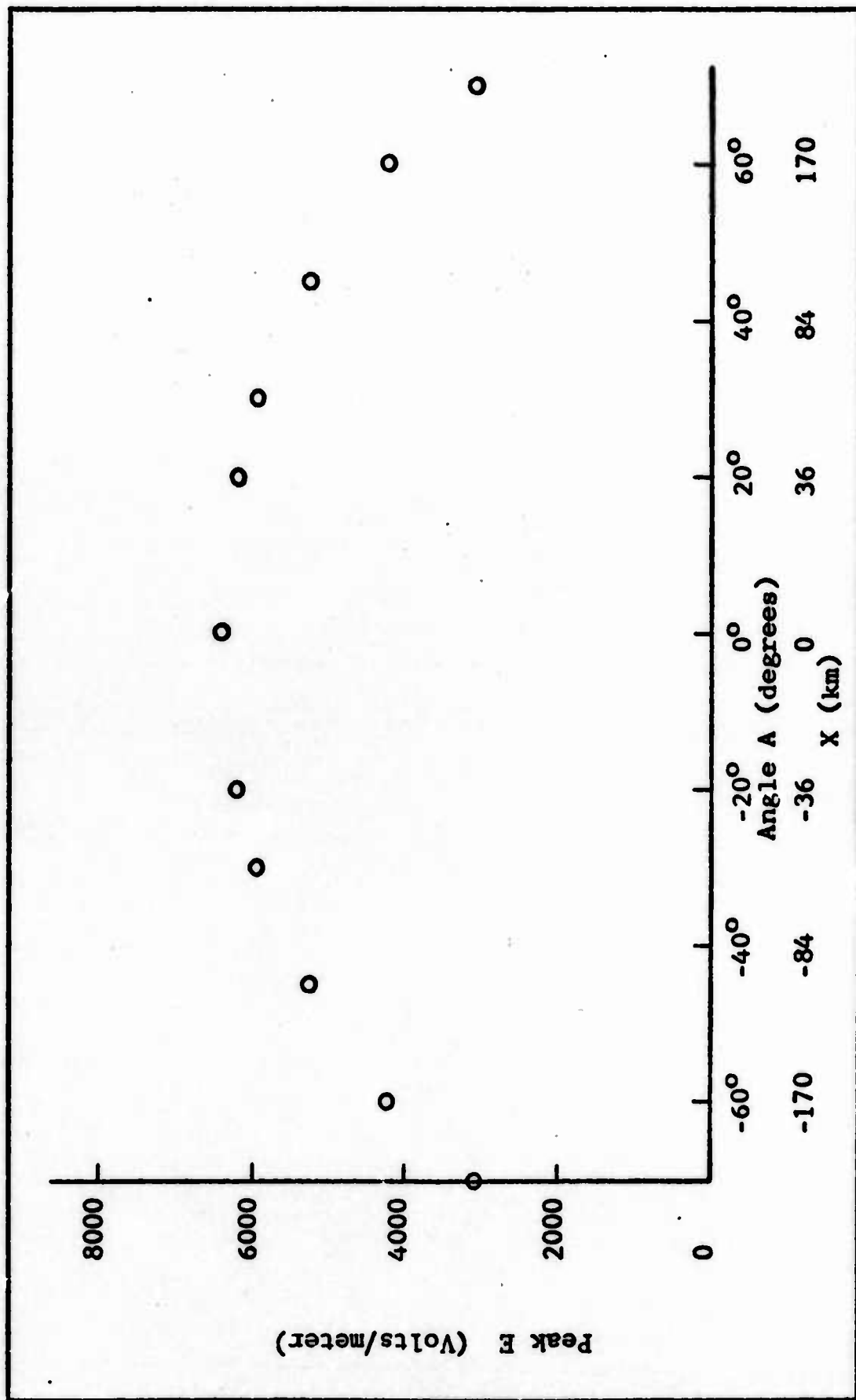


Fig. 6. Variation in the X Direction (Y=0, Z=0, HOB=100km, Y_γ=0.001kt)

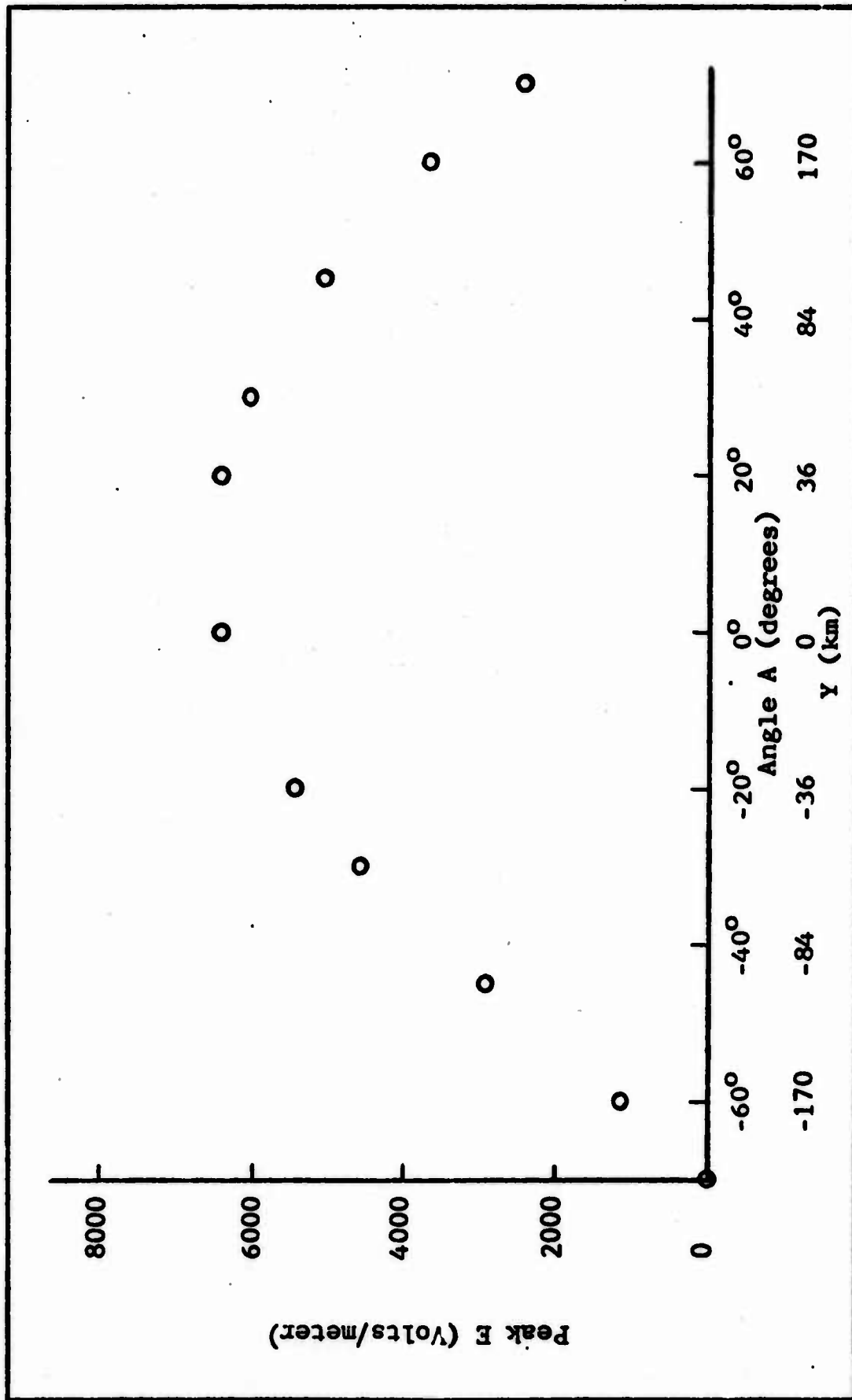


Fig. 7. Variation in Y direction (X=0, Z=0, HOB=100km, $\gamma_y = .001kt$)

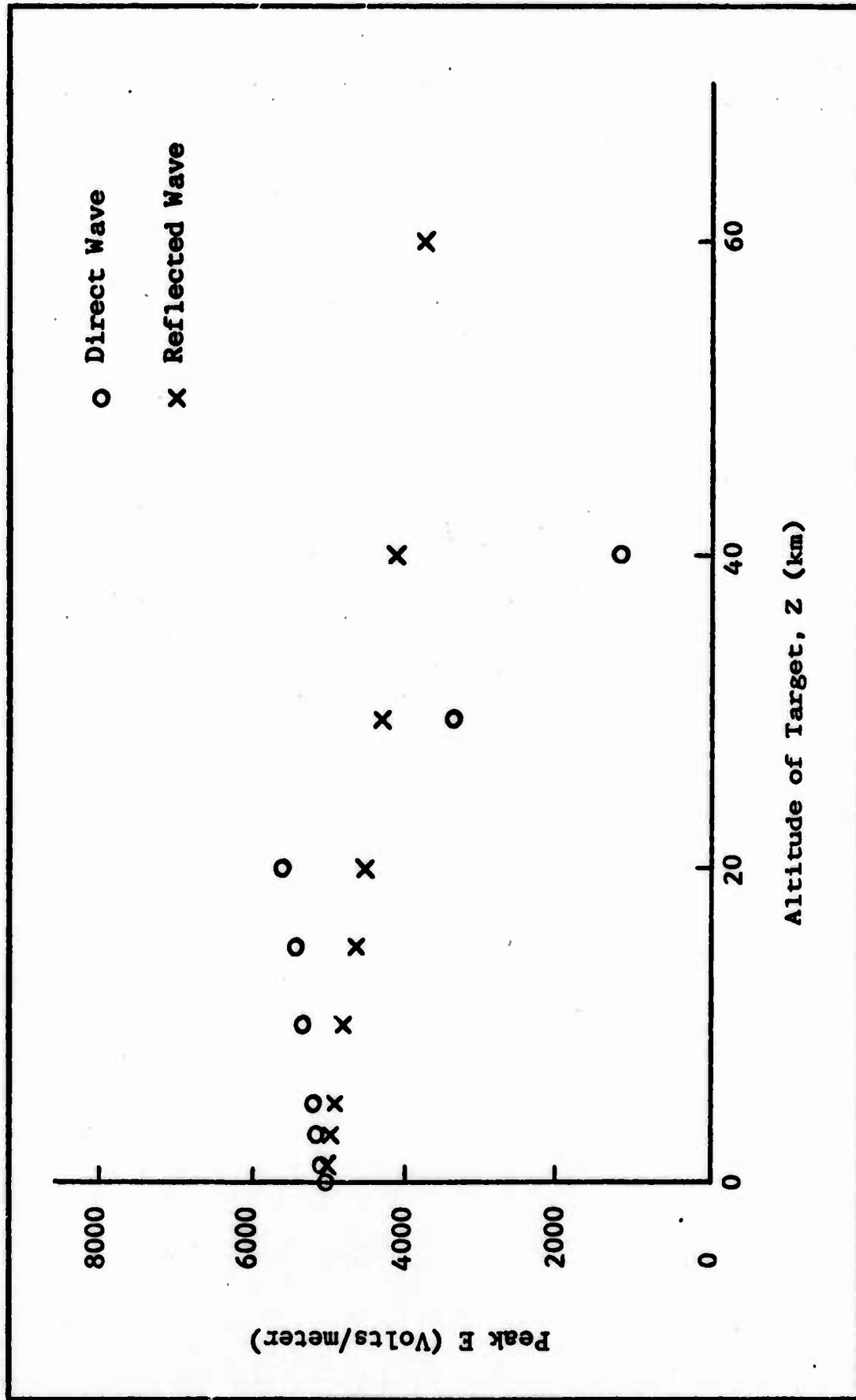


Fig. 8. Variation in Z Direction ($X=0$, $Y=100\text{km}$, $Y_Y=-.001\text{kt}$, $HOB=100\text{km}$)

region. Note that $Y = 100$ km for these runs. As expected, the direct wave falls off rapidly as the target altitude passes through the absorption region, since less of the absorption region contributes to the wave with each increase in altitude. The crossover point where the reflected wave becomes the largest occurred at 25 km in this case. Above ground zero the crossover point was 29.4 km. The altitude of the crossover point is both yield and geometry dependent. It is necessary for the user to calculate both waves whenever there is any doubt which one is the largest.

The reflected wave calculation assumes 100% reflection from the ground and no attenuation in the absorption region or the ionosphere. These assumptions are reasonable if it is recalled that only the high frequency component is being considered and that it requires at least

$$\frac{40 \text{ km}}{3(10)^8 \text{ m/sec}} = 133 \mu \text{ sec} \quad (67)$$

for the wave to leave the absorption region, reach the earth, be reflected, and return to the absorption region. This length of time is enough for a significant number of the free electrons to recombine and reduce the effective conductivity of the absorption region.

The results of variation in HOB are shown in Fig. 9. For all values of HOB attempted below 60 km the code went unstable. Infinite values for E were obtained which resulted in abnormal termination of the calculations. This is

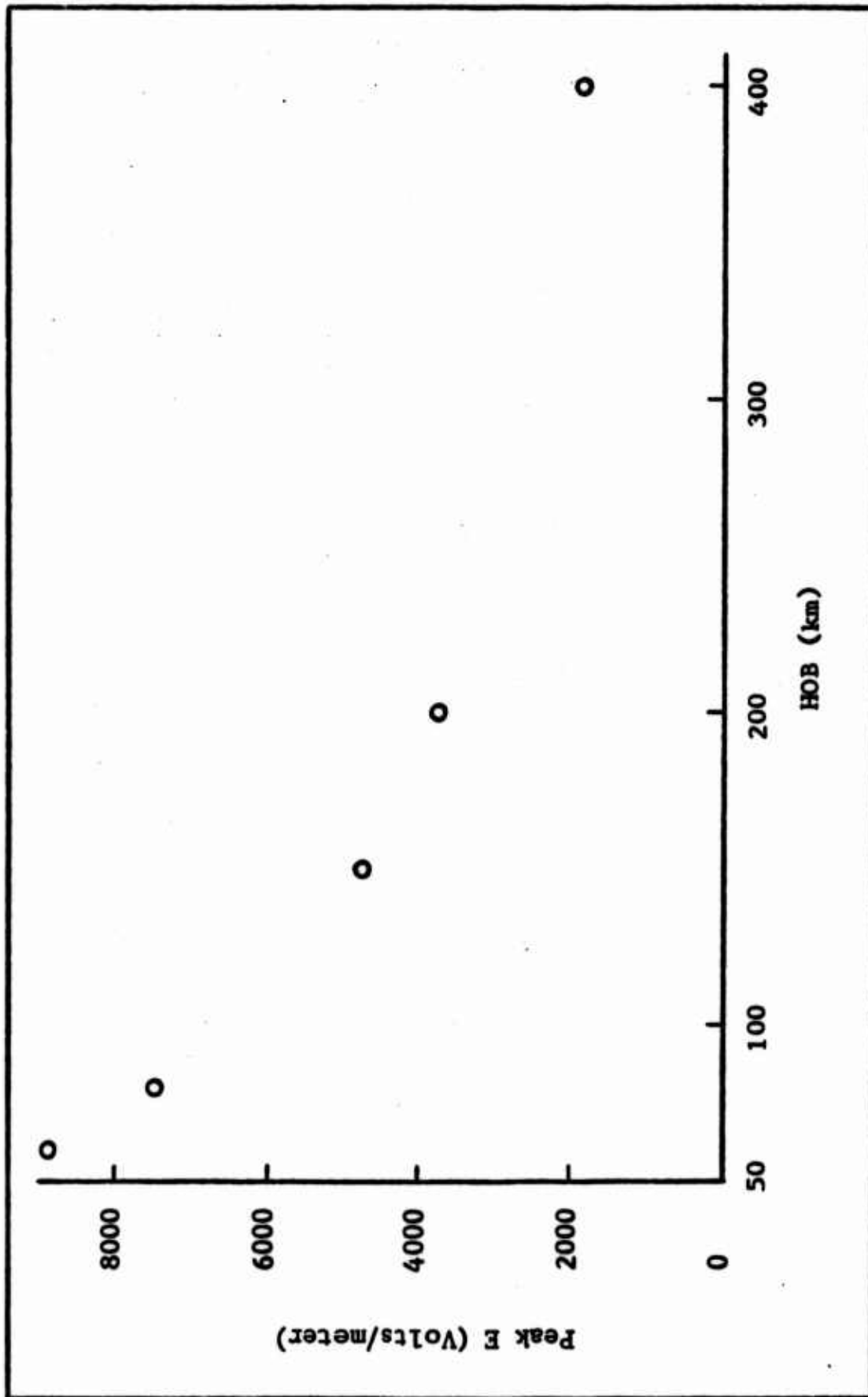


Fig. 9. Variation in Height of Burst ($X=0$, $Y=0$, $Z=0$, $Y_y=0.001kt$)

expected since the burst is assumed to be distant from the absorption region (equations 9 and 10).

The results of variation in gamma yield are shown in Fig. 10. For all gamma yields attempted above 60 tons the code went unstable, giving infinite values for E. However, the instability always occurred at times later than the natural peak value of E. For example, with 80 tons of gamma yield, the natural peak occurred at 1 shake and the instability occurred at 10 shakes. By using the natural peak value and ignoring the instability, reasonable values for peak E were obtained up to 1 kt of gamma yield.

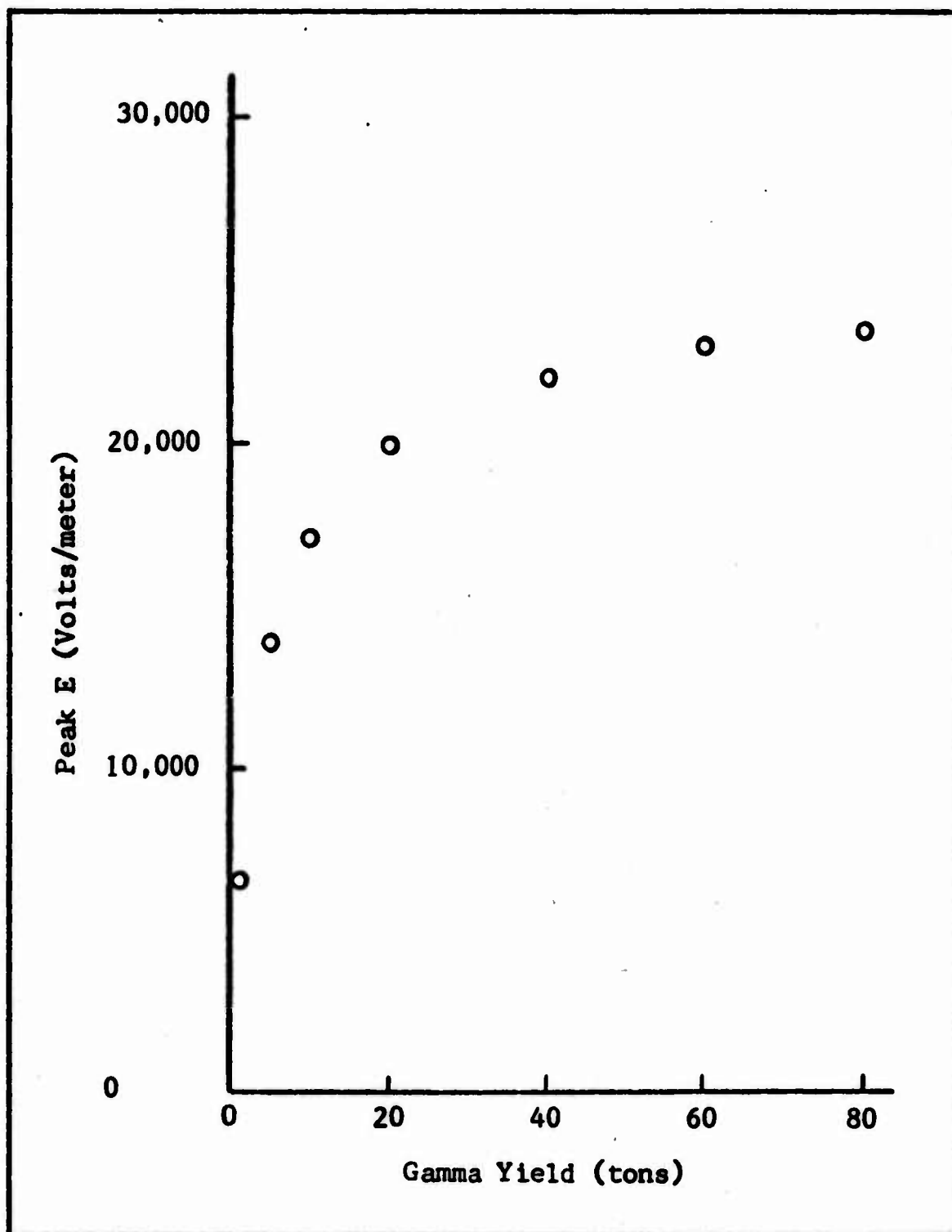


Fig. 10. Variation in Gamma Yield ($X=0$, $Y=0$, $Z=0$, HOB=100km)

V. Discussion and Recommendations

Limitations

Most of the limitations of the code are inherent in the model upon which it is based. Approximations such as a flat earth, a uniform magnetic field, and constant speed Compton electrons can be improved only by changing the model. In addition, the effect of the self generated electromagnetic fields on the motion of the Compton electrons is ignored, as is recombination of both primary and secondary electrons. The possibility of a single gamma ray interacting to produce more than one Compton electron is not allowed. In the absorption region the contribution of the non-propagating radial component of the electric field is neglected. Also, the model is not easily adapted to multi-group gamma transport, or to multiple burst calculations.

The code calculates only the effect of the gamma rays. The user must keep in mind that X-ray generated EMP becomes important for bursts above 100 km.

The code does not account for the increase in altitude of the absorption region for slant angles (angle A in Fig. 1) greater than 60° which is indicated by Latter and LeLevier (Ref 4).

Since 97% of the running time of the code is used for numerical iteration it is not practical to adapt the code to run more than one target at a time. Two targets would

merely double the running time, so it is simpler to just make two runs. Typical requirements are 200 seconds running time with 33000₈ words of central memory on the CDC 6600 computer using NDEL_R = 50 and TMAX = 20 shakes.

Uses

The code can be used to calculate the peak value of the E field at a target, anywhere on or above ground level, resulting from a nuclear burst above 60 km altitude with a gamma yield up to 60 tons. Either the direct or the ground reflected wave can be calculated. With special care, bursts up to 1 kt of gamma yield can be used.

Recommendations

In the interest of accuracy, the targets should be located such that the slant angle, A , is between -60° and $+60^\circ$.

By accepting a much longer running time the accuracy and hopefully, the stability of the code could be improved by using a smaller step size in the integration of the Compton current equations. Reducing the step size from one tenth of the Compton lifetime to one shake would require approximately ten times as much running time as the code presently requires. This possibility should be investigated further to determine the optimum step size for obtaining the best relationship between accuracy and running time.

Another possibility for increasing the accuracy and stability of the code is to reduce the step size in r . The present code has the capability of dividing the absorption region into 500 steps in r along the line of sight. Of course, the running time required for 500 steps is ten times that required for 50 steps. A modification of the code to allow more than 500 steps would increase the amount of computer core required as well as increasing the running time. This provides another area for investigation to determine the best trade off point between accuracy and running cost.

These two possibilities could be investigated with minor modifications to the present code. However, the computer time required would be considerable.

In addition, there are numerous possibilities for improvements in the model itself. Some of the more important ones are;

Using multigroup gamma transport.

Using multigroup Compton electrons.

Allowing angular distribution of Compton electrons.

Using self consistent electromagnetic fields.

Including the low frequency components.

Each of these would require major modifications to the present code.

Bibliography

1. Kinsley, O.V. Introduction to the Electromagnetic Pulse, Wright-Patterson AFB: Air Force Institute of Technology, March 1971. (GNE/PH/71-4).
2. Karzas, W. J. and R. Latter. "Detection of the Electromagnetic Radiation from Nuclear Explosions in Space", Physical Review, Vol 137, No. 5B. pages 1369-1378, March 8, 1965. (Also published as EMP Theoretical Note 40).
3. Pomranning, G. C. "Early Time Air Fireball Model for a Near-Surface Burst", DNA 3029T, March 1973.
4. Latter, R. and R. E. LeLevier. "Detection of Ionization Effects from Nuclear Explosions in Space", Journal of Geophysical Research, Vol. 68, No. 6, March 15, 1963.
5. Wylie, C. R. Jr. Advanced Engineering Mathematics, New York: McGraw-Hill Book Co. 1966. (Third Edition).
6. Lecture Notes, Electromagnetic Waves, EE 6.30, Air Force Institute of Technology, Wright-Patterson AFB, Summer, 1973. (Course taught by Maj. Carl T. Case.)

Appendix A

EMP Code User's Guide

EMP Code User's Guide

The code is run the same as any other Fortran Extended program, but due to the running time it should be converted to binary form before execution. The plotting subroutine requires an on-line plotter and both linear and log plotting library subroutines.

The input data is read in the following order:

Data card #1, using FORMAT (7F10.0, 215), contains;

X,Y,Z The target coordinates in meters
 HOB The height of the burst in kilometers
 (60 km \leq HOB)
 GAMYLD The gamma yield in kilotons
 (GAMYLD \leq 1 kt)
 BFIELD The Earth's magnetic field in wb/m²
 BANGLE The magnetic field dip angle in degrees
 NDELR The number of steps in r taken through
 the absorption region (50 \leq NDELR \leq 500)
 OUT The output control parameter

Data card #2, using FORMAT (13), contains;

ITER The time period covered by the iterations
 in shakes (10 \leq ITER \leq 100) (ITER = TMAX)

Data card #3, using FORMAT (4F10.0), contains;

A Pomranning constant α in inverse shakes
 B Pomranning constant β in inverse shakes
 RN Pomranning constant N in shakes
 TO Pomranning constant τ_0 in shakes

Default values are provided for BANGLE, BFIELD, and NDELR. They are 40° , 0.00002 wb/m^2 , and 50 respectively. If these default values are desired, zero must be punched in their respective card fields.

The ground reflected wave at the target is obtained by reading in the target altitude, Z, as a negative number. For any target within the absorption region, both the direct and the ground reflected wave should be calculated to determine which one is the strongest.

For values of GAMYLD between 0.06 kilotons and 1.0 kilotons the code will most likely go unstable. This instability occurs after the real peak has been calculated, but the peak value printed out may not be the real peak. Since execution is terminated when the field becomes greater than $1\text{E}15 \text{ V/m}$, the array search can result in a false peak value. In this case, the array itself (or the plot) can be used to determine the real peak value.

Increasing NDELR makes the step size in r through the absorption region smaller and the calculation becomes more accurate. However, total running time varies directly with changes in NDELR. For example, using NDELR = 100 instead of NDELR = 50 will approximately double the running time required for NDELR = 50.

There are four output options provided. Option 0 prints out the informative messages, the calculated peak value at the target, the E array, and the τ array. Option 1 adds a linear plot of the first 20 shakes and a log-log

plot of 100 shakes of E as a function of τ at the target. Option 2 includes both Option 0 and Option 1 and adds a printout of E and σ as a function of τ at the bottom of the absorption region. Option 3 deletes the plots from Option 2. The last two options are primarily for debugging since a partial printout is made for each completed iteration even if execution is terminated before the iterations are completed. The first two options are best for production runs.

The only requirements on the Pomranning constants are N must be chosen such that equations (61) and (62) are satisfied, all of them must be positive, and $\alpha > \beta$.

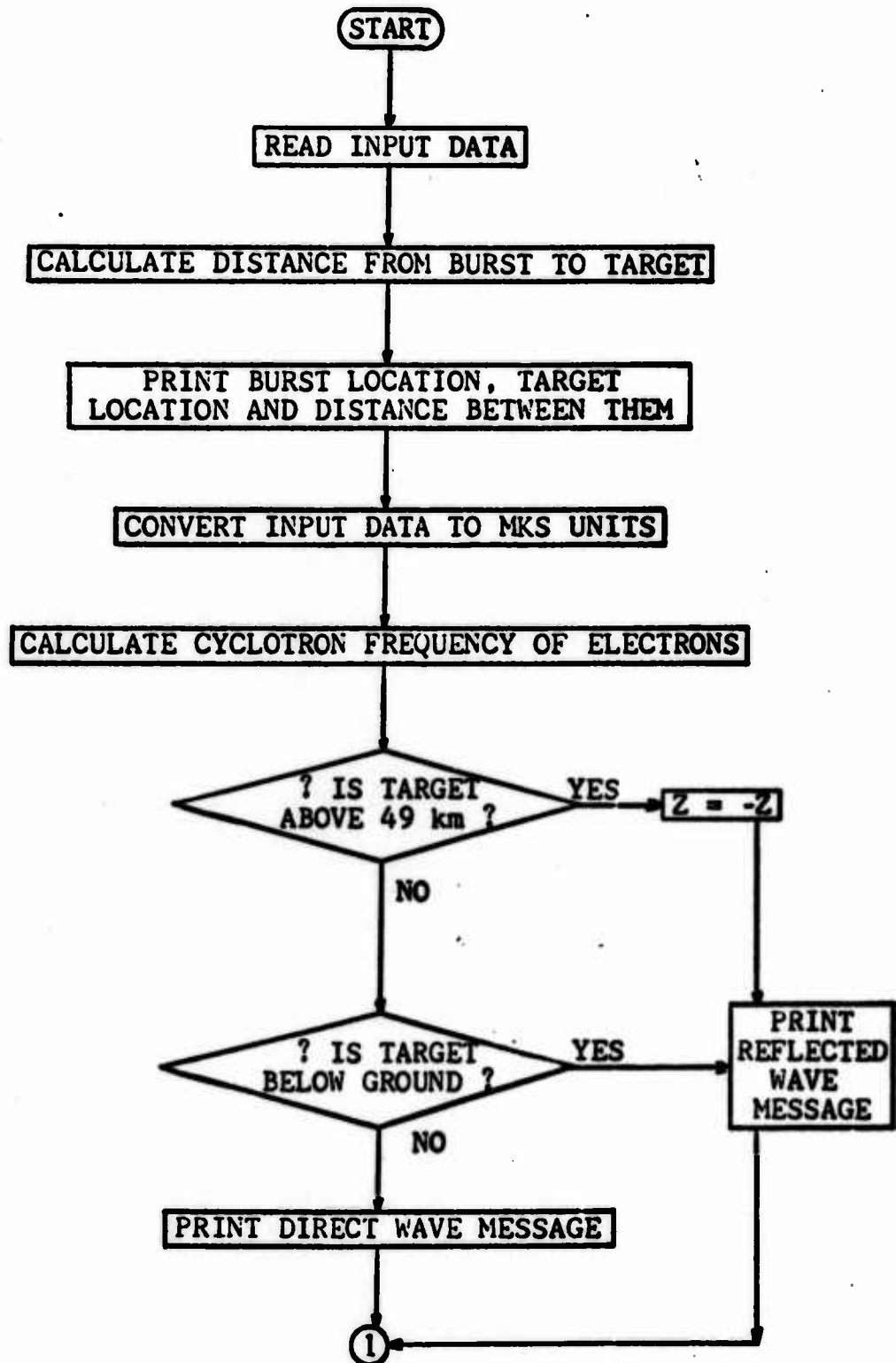
Increasing ITER also increases the running time. For ITER = 10 shakes, running time is approximately 180 seconds on the CDC 6600 computer. For ITER = 100 shakes, running time is approximately 340 seconds. A good compromise, which gives nice looking plots, is ITER = 20 shakes with a running time of approximately 200 seconds.

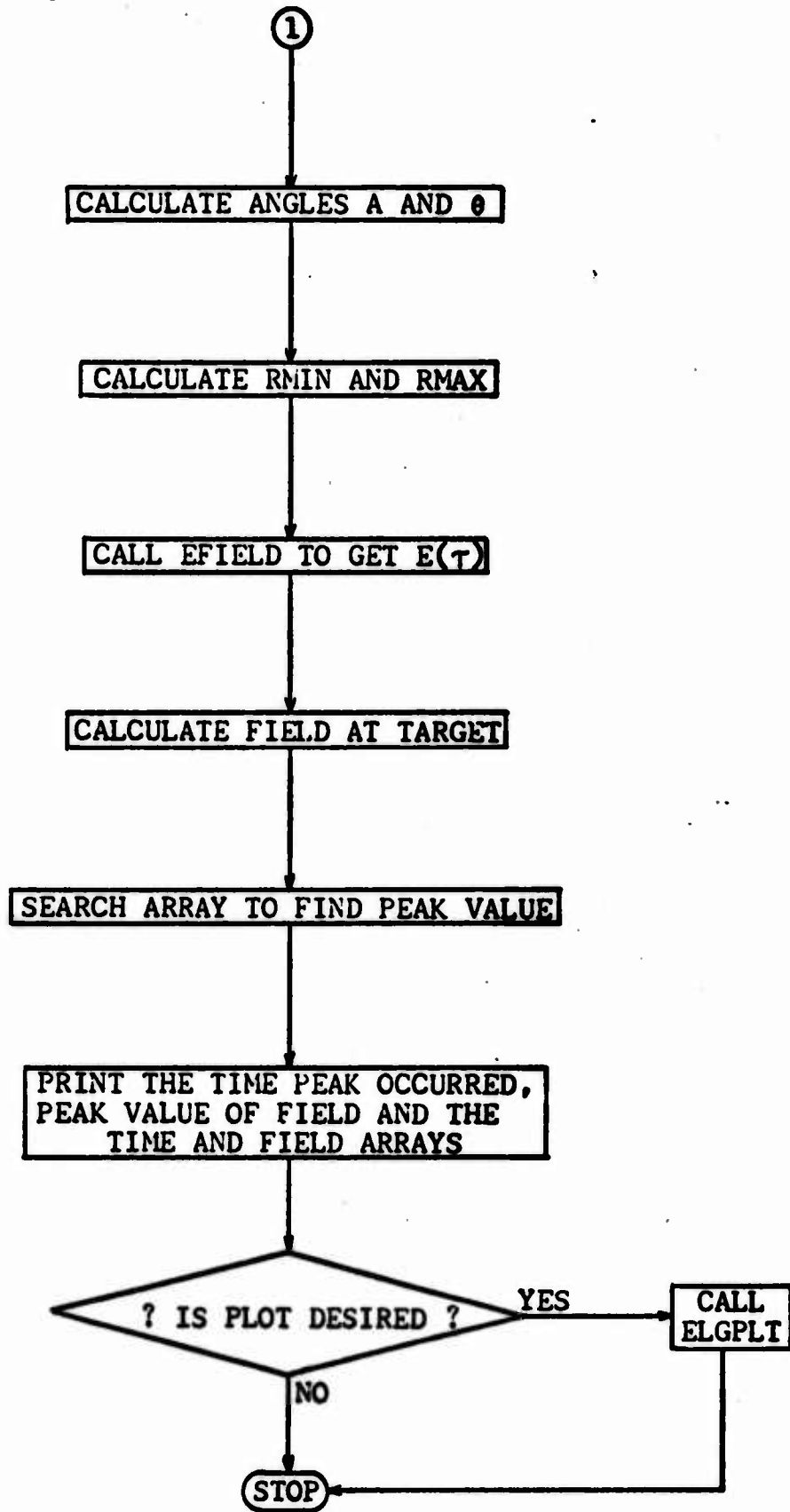
In binary form, the code requires 33000₈ words of core on the CDC 6600 computer.

Appendix B

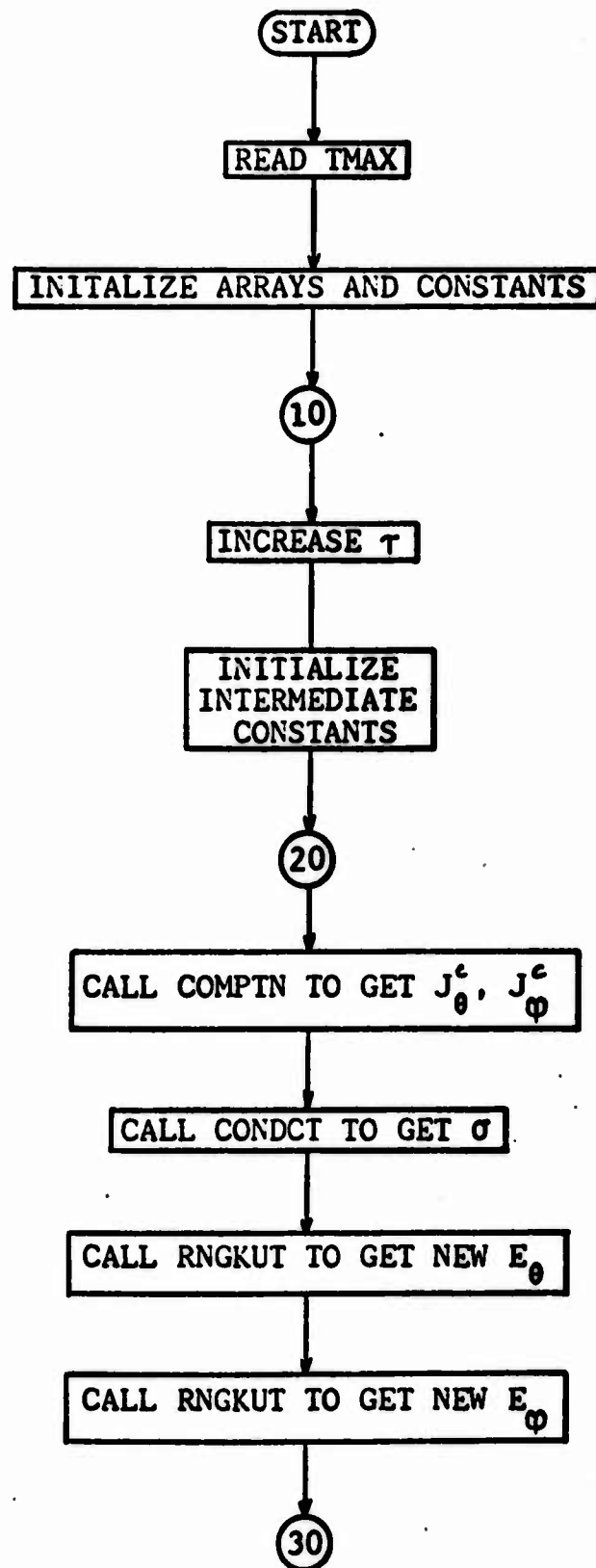
EMP Code Flow Charts

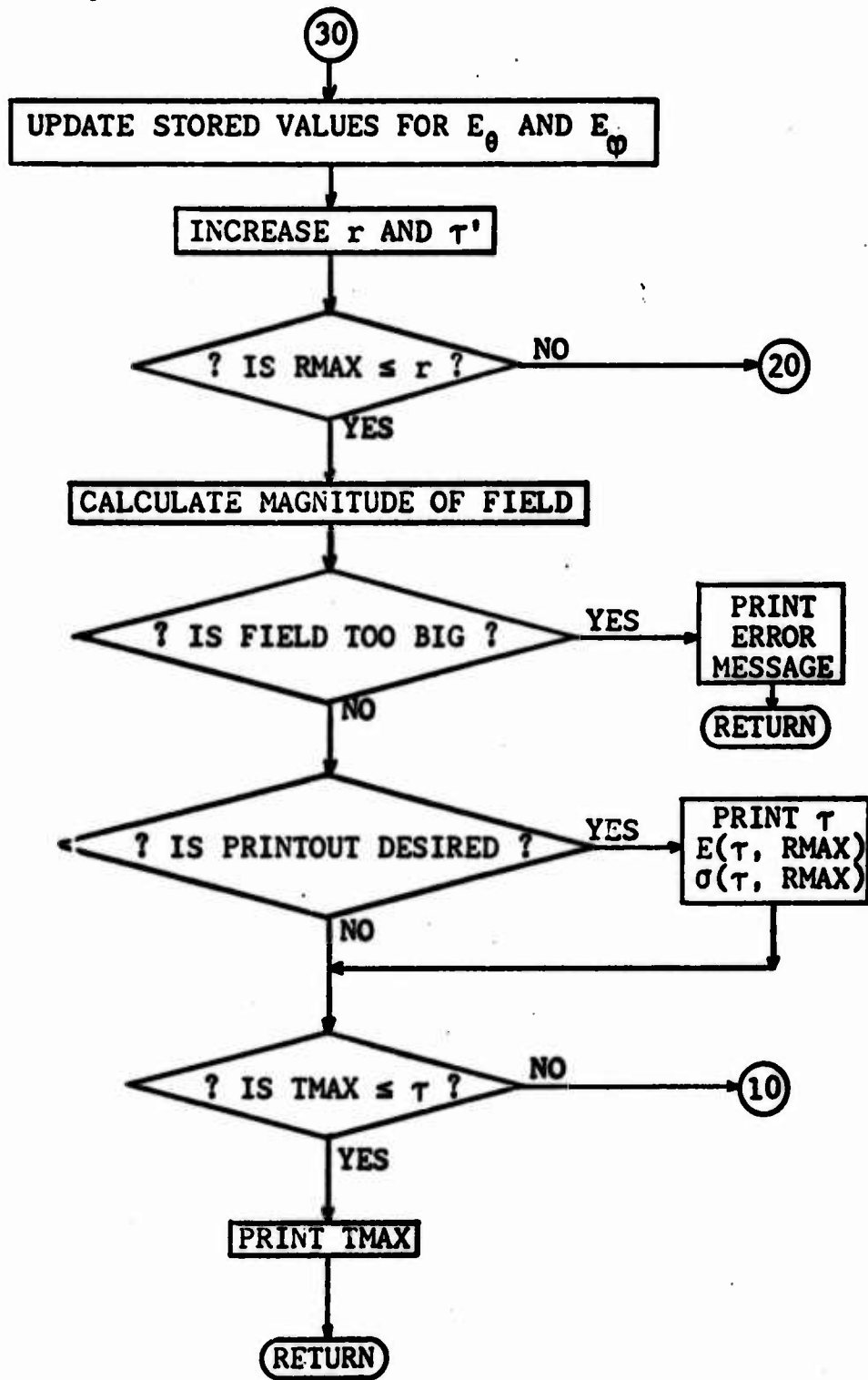
PROGRAM CONTRL



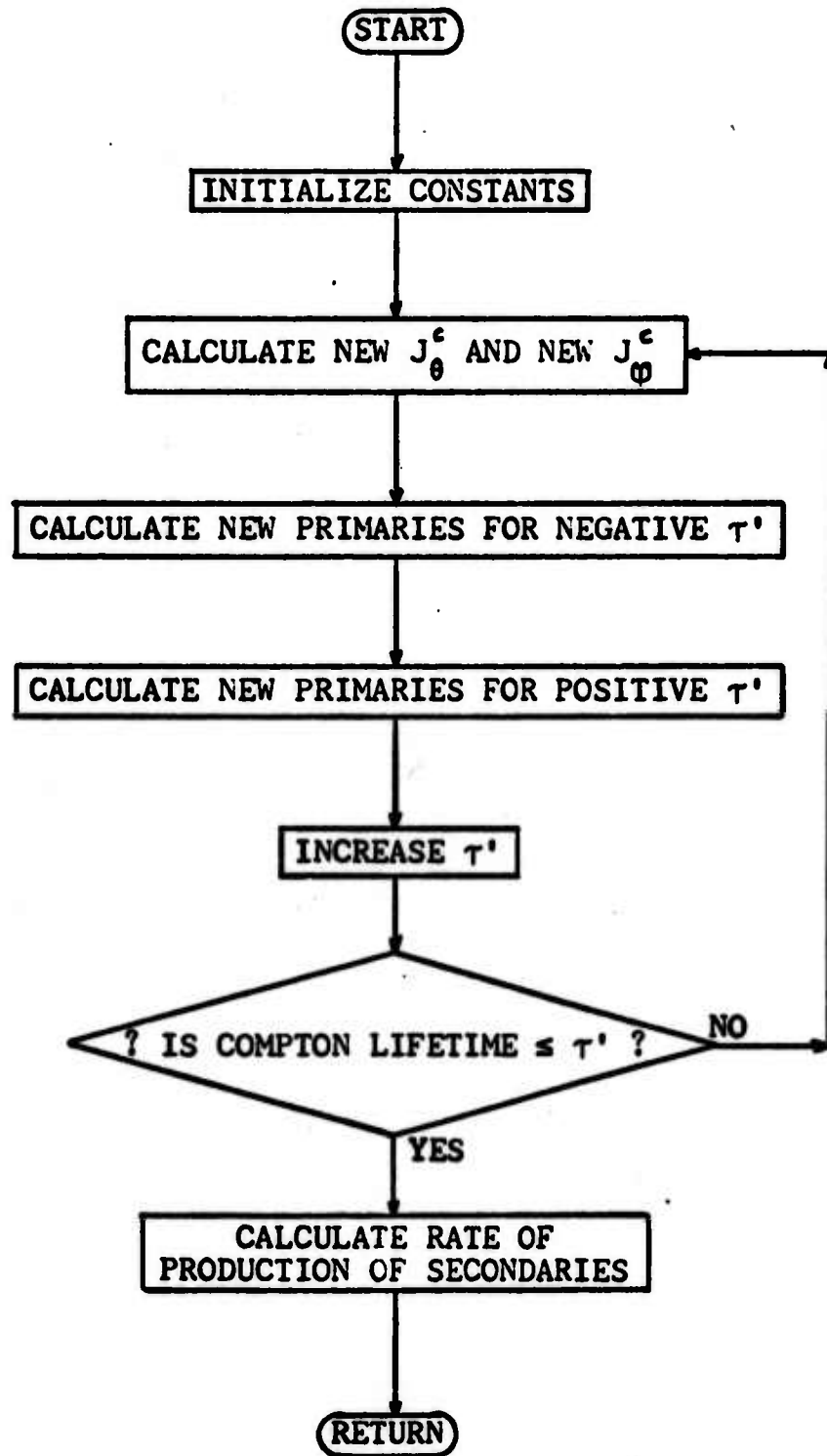


SUBROUTINE EFIELD

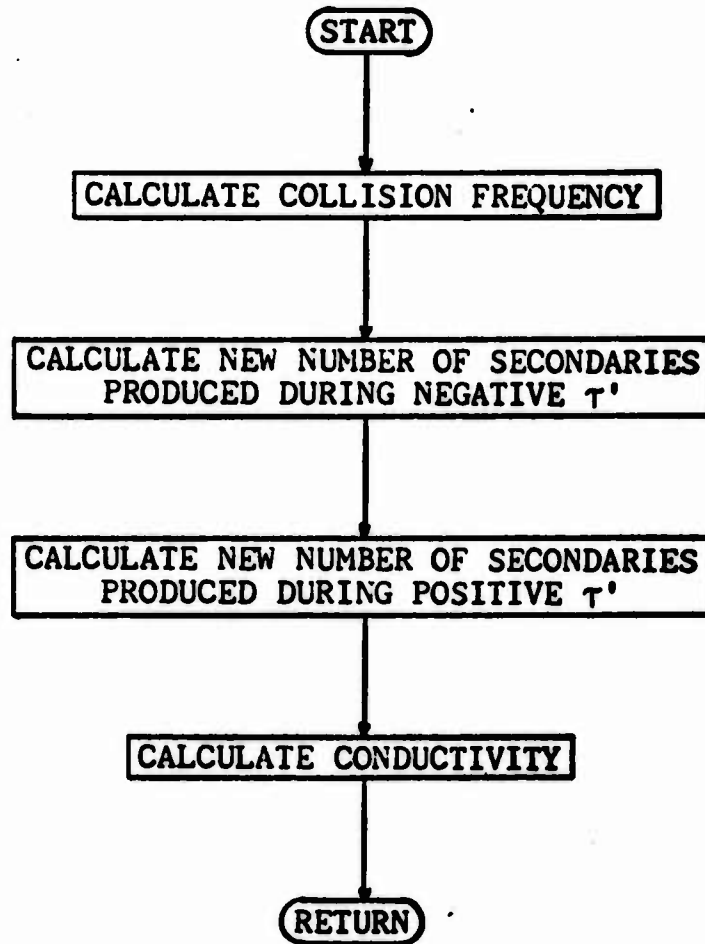




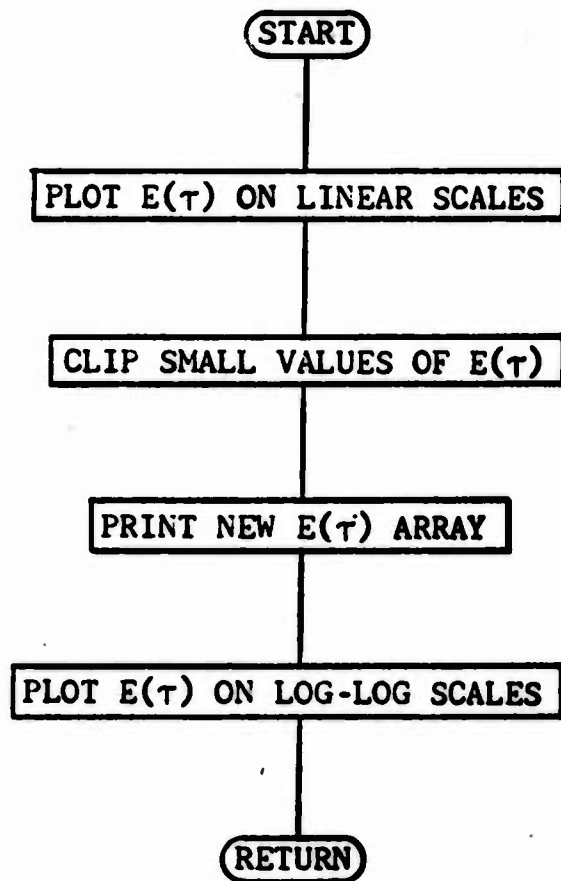
SUBROUTINE COMPTN



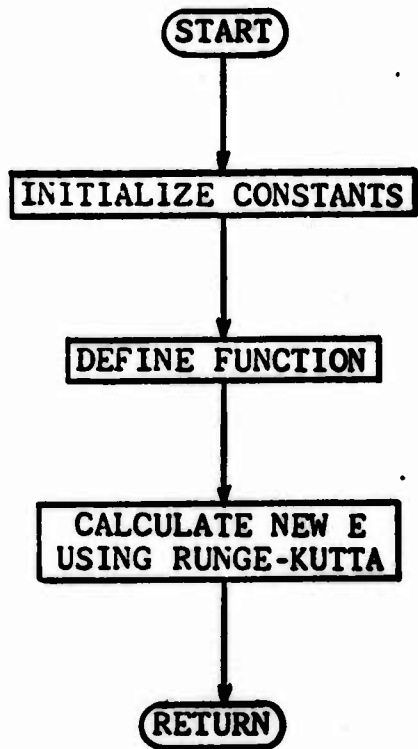
SUBROUTINE CONDCT



SUBROUTINE ELGPLT



SUBROUTINE RNGKUT



Appendix C

EMP Code Listing

CNTL 10
 CNTL 20
 CNTL 30
 CNTL 40
 CNTL 50
 CNTL 60
 CNTL 70
 CNTL 80
 CNTL 90
 CNTL 100
 CNTL 110
 CNTL 120
 CNTL 130
 CNTL 140
 CNTL 150
 CNTL 160
 CNTL 170
 CNTL 180
 CNTL 190
 CNTL 200
 CNTL 210
 CNTL 220
 CNTL 230
 CNTL 240
 CNTL 250
 CNTL 260
 CNTL 270
 CNTL 280
 CNTL 290
 CNTL 300
 CNTL 310
 CNTL 320
 CNTL 330
 CNTL 340
 CNTL 350
 CNTL 360

```

PROGRAM CONTROL (INFLU, CLTFLCT, FLOT)
C
C
C
THIS PROGRAM CONTROLS THE SUBROUTINES
C
COMMON OUT
INTEGER CUT
DIMENSION E(192), TIME(192), STORE2(500)
C
X, Y, Z IS THE TARGET LOCATION IN METERS
FOR THE NORTHERN HEMISPHERE
X IS MAGNETIC WEST
Y IS MAGNETIC SOUTH
Z IS ALTITUDE
C
HOB IS HEIGHT OF BURST IN KILOMETERS > 50KM
C
GAMMAD IS GAMMA YIELD OF BURST IN KILOCICNS
C
BFIELD IS THE MAGNITUDE OF EARTH'S MAGNETIC FIELD IN THE
ABSORPTION REGION BELOW THE BURST IN WEBERS/SQUARE METER
C
BANGLE IS THE DIP ANGLE OF THE MAGNETIC FIELD IN DEGREES
C
NDELRL IS THE NUMBER OF STEPS BETWEEN RMIN AND RMAX
50<=NDELRL<=500
C
OUT IS THE OUTPUT CONTROL PARAMETER
OUT=0 ==> PRINT PEAK VALUE AND ARRAYS
OUT=1 ==> PRINT PEAK VALUE AND MAKE FLCT
OUT=2 ==> PRINT EVERYTHING AND MAKE FLCT
OUT=3 ==> PRINT EVERYTHING
C
READ 1001, X, Y, Z, HOB, GAMMAD, EFFELD, BANGLE, NDELRL, OUT
F=SQRT(X**2+Y**2+(HOB**2)**2)
PRINT 2006, GAMMAD, HOB, X, Y, Z, F
C
  
```

CNTL 370
 CNTL 380
 CNTL 390
 CNTL 400
 CNTL 410
 CNTL 420
 CNTL 430
 CNTL 440
 CNTL 450
 CNTL 460
 CNTL 470
 CNTL 480
 CNTL 490
 CNTL 500
 CNTL 510
 CNTL 520
 CNTL 530
 CNTL 540
 CNTL 550
 CNTL 560
 CNTL 570
 CNTL 580
 CNTL 590
 CNTL 600
 CNTL 610
 CNTL 620
 CNTL 630
 CNTL 640
 CNTL 650
 CNTL 660
 CNTL 670
 CNTL 680
 CNTL 690
 CNTL 700
 CNTL 710
 CNTL 720

```

C C SET UP DEFAULT VALUES
C C IF(BANGLE.EQ.0.) BANGLE=40.
C C IF(RFIELD.EQ.0.) RFIELD=0.00002
C C IF(NDELR.EQ.0) NDELR=50
C C CONVERT DATA TO MKS UNITS
C C HCR=HOB*1000.
C C GAMYLD=2.61625E25*GAMYLC
C C BANGLE=0.017453295*EANGLE
C C MEGA=1.6E-19*RFIELD/(3.50E*%11E-31)
C C PRINT TYPE OF CALCULATION
C C REFLCT=49000.
C C IF(Z.GT.REFLCT)PRINT 2007
C C IF(Z.LT.0.0) PRINT 2008
C C IF(Z.LE.REFLCT.AND.Z.GE.C.(.) PRINT 2009
C C REFLECTED WAVE CALCULATION ASSUMES 100% REFLECTION
C C AND USES MIRROR IMAGE CF TARGET BELOW GROUND
C C SET Z = -Z IF REFLECTED WAVE IS TO BE USED
C C IF(Z.GT.REFLCT) Z=-Z
C C IF(Z.GT.HOB-1000.) PRINT 2007
C C IF(Z.GT.HOB-1000.) Z=-Z
C C DETERMINE ANGLES
C C R=SQRT(X*X+Y*Y+(HOB-Z)**2)
C C A=ACOS((HOB-Z)/R)
C C THETA=ACOS(COS(BANGLE)*Y/R+SIN(BANGLE)*(Z-HOB)/R)
C C DETERMINE RMIN AND RMAX
  
```


Reproduced from
best available copy.

CNTL1090
CNTL1100
CNTL1110
CNTL1120
CNTL1130
CNTL1140
CNTL1150
CNTL1160
CNTL1170
CNTL1180
CNTL1190
CNTL1200
CNTL1210
CNTL1220
CNTL1230
CNTL1240
CNTL1250
CNTL1260
CNTL1270
CNTL1280
CNTL1290
CNTL1300
CNTL1310
CNTL1320
CNTL1330
CNTL1340
CNTL1350
CNTL1360

```

PRINT 2001
PRINT 2002, (TIME(I), I=1, 190)
PRINT 2003
PRINT 2004, (E(I), I=1, 190)

C
C IF DESIRED, MAKE FLCT
C
IF(OUT.LE.0.CR.OUT.(GE.3) STCF
CALL ELGFLT (E, TIME, RIG)
STOP
1001 FCRMAT(7F10.0, 2I5)
2010 FCRMAT(/5X, "PEAK OCCUFRED AT", F5.1, " SHAKES"//)
2009 FCRMAT(5X, "DIRECT WAVE IS BEING CALCULATED"//)
2008 FCRMAT(5X, "REFLECTED WAVE IS BEING CALCULATED"//)
2007 FCRMAT(5X, "TARGET IS ABOVE ASCRIPTION REGION SO REFLECTED WAVE IS
1PEING CALCULATED"//)
2006 FCRMAT("1 THE BURST WITH GAMMA YIELD CF", 1PE10.3, " KILOTCNS"
1 /5X, "IS AT AN ALTITUDE CF", 1PE10.3, " KILOMETERS."
2 //5X, "THE TARGET IS AT CCORDINATES", 3(5X, 1PE10.3)
3 /5X, "WHICH IS", 1PE10.3, " METERS FRCP THE BURST"//)
2005 FCRMAT(/5X, "1 /5X, "2 PEAK EFIELD AT TARGET IS ", 1PE10.3, " VOLTS/METER "
1 /5X, "2 /5X, "3 TIMES USED (IN SHAKES) ARE"//)
2004 FCRMAT(19(10(3X, 1PE10.3)))
2003 FCRMAT(/5X, "EFIELD VALLES AT TARGET (IN V/M) ARE"//)
2002 FCRMAT(19(10(4X, F5.1, 4X)))
2001 FCRMAT("1 TIMES USED (IN SHAKES) ARE"//)
END
    
```


EFLL 730
 EFLL 740
 EFLL 750
 EFLL 760
 EFLL 770
 EFLL 780
 EFLL 790
 EFLL 800
 EFLL 810
 EFLL 820
 EFLL 830
 EFLL 840
 EFLL 850
 EFLL 860
 EFLL 870

```

52      PRINT 301
        PRINT 201,TIME(IT)
        IF(IT.LT.10)RETURN
C
C      SET LAST 5 VALUES OF EFIELD TO 0.0 TO AVOID INCORRECT PEAK
C
        E(IT)=E(IT-1)=E(IT-2)=E(IT-3)=E(IT-4)=E(IT-5)=0.0
        RETURN
        FCRMAT (I3)
        FCRMAT(" I =",I4," TIME =",F6.1," SHAKES E(T,RMAX) =",
11FE10.3," VOLTS/METER SIGMA =",1PE10.3," MHO/METER")
        FCRMAT("//5X,"ITERATION TERMINATED AFTER",F5.1," SHAKES"//)
        FCRMAT("//15X,"*****"/15X,"***** SOLUTIONICN HAS GONE UNSTABLE"
1/15X,"*****"//)
        END
    
```

CNCT 10
 CNCT 20
 CNCT 30
 CNCT 40
 CNCT 50
 CNCT 60
 CNCT 70
 CNCT 80
 CNCT 90
 CNCT 100
 CNCT 110
 CNCT 120
 CNCT 130
 CNCT 140
 CNCT 150
 CNCT 160

```

SUBROUTINE CCNDCT(SIGMA,FFI,CTP,DT,HOB,R,A,STORE1,STORE2,K,NCELR,
1FPI2)
C
C      CALCULATES SIGMA AFTER FINDING
C      NSECNDARY FROM NPRIMARY
C
        STCR21 CCNTAINS INTEGRAL FOR NEGATIVE TAU
        STCR22 CCNTAINS INTEGRAL FOR POSITIVE TAU
C
        DIMENSION STCR2(NDLELR)
        CCLISN=4.E12*EXP((R*CCS(A)-PCB)/7000.)
        STORE1=STCR21-PTF
        STCR2(K)=STCR2(K)+PRI2*CT*(1.0E-9)
        SEC=STCR2(K)-STORE1
        SIGMA=(1.6E-19**2)*SEC/(CCLISN*9.11E-31)
        RETURN $ END
    
```


CMTN 370
 CMTN 380
 CMTN 390
 CMTN 400
 CMTN 410
 CMTN 420
 CMTN 430
 CMTN 440
 CMTN 450
 CMTN 460
 CMTN 470
 CMTN 480
 CMTN 490
 CMTN 500
 CMTN 510
 CMTN 520
 CMTN 530
 CMTN 540
 CMTN 545
 CMTN 550
 CMTN 560
 CMTN 570
 CMTN 580

JPHI=JPHI+(PK5+2.*(RK6+RK7)+RK8)/6.

RUNGE-KUTTA INTEGRATION OF PRIMARIES

RKP1=DT*RKCMTN(R,THETA,OMEGA,TP,TPRIME)
 RKP2=DT*RKCMTN(R,THETA,OMEGA,TP,TPRIME+H)
 RKP3=RKP2
 RKP4=DT*RKCMTN(R,THETA,OMEGA,TP,TPRIME+DT)
 PKI=PRI+(RKFI+2.*(RKP2+RKP3)+RKP4)/6.
 RP1=DT*PKCMTN(R,THETA,CMEGA,T,TPRIME)
 RP2=DT*PKCMTN(R,THETA,OMEGA,T,TPRIME+H)
 RP3=RP2
 RP4=DT*PKCMTN(R,THETA,CMEGA,T,TPRIME+DT)
 PRI2=PRI2+(RP1+2.*(RP2+RP3)+RP4)/6.
 TPRIME=TPRIME+DT

31

CONTINUE

MULTIPLY PRIMARIES BY O*G(R)/THAX
 TO OBTAIN RATE OF PRODUCTION OF SECONDARIES

PRI=PRI+5.000E4*GOFR(R,A,HOB,PATH,GAMYLD)/THAX
 PRI2=PRI2+5.0E4*GOFR(R,A,HOB,PATH,GAMYLD)/THAX
 RETURN \$ END

C
 C
 C

C
 C
 C
 C

CMPT1010
 CMPT1020
 CMPT1030
 CMPT1040
 CMPT1050
 CMPT1060
 CMPT1070
 CMPT1080
 CMPT1090
 CMPT1100

```

FUNCTION CMPTI(HOR,F,A,THETA,OMEGA,PATH,T,TPRIME,GAMYLD)
C
C
C
C
    CALCULATES F(T,F) FCF FLNGE-KUTTA INTEGRATION
    OF PHI COMPONENT OF CCFTON CURRENT
    SOLVE=TOFT(T,TPRIME,THETA,CMEGA)
    SOLVE=FOFT(SOLVE)
    SOLVE=SOLVE+(-4.608E-11)*GCFF(R,A,HOB,FATH,GAMYLD)
    CMPTI=SOLVE+SIN(THETA)*SIN(CMEGA*TPRIME)
    RETURN $ END
    
```

C
 C
 C
 C

CMTT1010
 CMTT1020
 CMTT1030
 CMTT1040
 CMTT1050
 CMTT1060
 CMTT1070
 CMTT1080
 CMTT1090
 CMTT1100

```

FUNCTION CMTTET(HOE,R,A,THETA,OMEGA,PATH,T,TPRIME,GAMYLD)
C
C
C
C
    CALCULATES F(T,F) FCF FLNGE-KUTTA INTEGRATION
    OF THETA COMPONENT OF CCFTON CURRENT
    SOLVE=TOFT(T,TPRIME,THETA,CMEGA)
    SOLVE=FOFT(SOLVE)
    SOLVE=SOLVE+(-4.608E-11)*GCFF(R,A,HOB,FATH,GAMYLD)
    CMTTET=SOLVE+SIN(THETA)*COS(CMEGA*TPRIME)-1.0)
    RETURN $ END
    
```

C
 C
 C
 C

RNKT1010
 RNKT1020
 RNKT1030
 RNKT1040
 RNKT1050
 RNKT1060
 RNKT1070
 RNKT1080
 RNKT1090
 RNKT1100
 RNKT1110
 RNKT1120
 RNKT1130

SUBROUTINE RANGKIT (E1,E,F,t,SIGMA,COMPTJ)

C
 C
 C
 C

E(I+1) IS CALCULATED FFCT E(I)
 USING THE RUNGE-KUTTA METHOD

DATA (C=3.0E2), (RMLC=12.5E-37E-7)
 EFUN(R,E)=- (1./R+C*FMUO+SIGMA/2.)*E-COMPTJ*C*RMUO/2.
 FK1=H*EFUN(P,E)
 RK2=H*EFUN(R+H/2.,E+PK1/2.)
 RK3=H*EFUN(R+H/2.,E+RK2/2.)
 RK4=H*EFUN(R+H,E+RK3)
 E1=E+(RK1+2.*(RK2+RK3)+RK4)/6.
 RETURN \$ END

FKCP1010
 FKCP1020
 FKCP1030
 FKCP1040
 FKCP1050
 FKCP1060
 FKCP1070
 FKCP1080

FUNCTION RKCPN(R,THETA,CMEGA,TP,TPRIME)

C
 C
 C
 C

CALCULATES F(T) FOR RUNGE-KUTTA
 INTEGRATION OF PRIMARY ELECTRONS

SOLVE=TOFT(TF,TPRIME,THETA,CMEGA)
 RKCPN=FCFT(SOLVE)
 RETURN \$ END

GCFF1010
 GOFR1020
 GCFF1030
 GCFF1040
 GOFR1050
 GCFF1060
 GOFR1070
 GCFF1080
 GOFR1090

FUNCTION GOFF (R,A,POF,FATH,GAMYLD)

SOLVES VIRGIN TRANSFCRT AND USES REACTION RATE TO
 CALCULATE THE NUMPER DENSITY OF RACIAL ELECTRONS

SOLVE=(.0226275/COS(A))*(-1.+EXP(R*COS(A)/7000.))*EXP(-HOB/7000.)
 DENOM=12.56637*P*R*FATH*1.5
 GCFF=EXP(-SOLVE)*GAMYLD/CENCF
 RETURN \$ END

C
 C
 C
 C

CLTF1010
 CLIF1020
 CLIF1030
 CLIF1040
 CLIF1050
 CLIF1060
 CLIF1070
 CLIF1080
 CLIF1090

FUNCTION CLIFE (R,A,HOP)

CALCULATES COMFTCN LIFETIME AT RADIUS = R
 MAX ACCEPTABLE LIFETIME = 100 SHAKES FCR
 THE KAPZAS-LATTER HIGH FREQUENCY AFFRCX

CLIFE=1.041667E-8*EXP((PCE-R*CCS(A))/7000.)
 IF(CLIFE.GT.1.E-6) CLIFE=(1.E-6)
 RETURN \$ END

C
 C
 C
 C
 C

FJFT101J
 FJFT102J
 FJFT103J
 FJFT104J
 FJFT105J
 FJFT106J
 FJFT107J
 FJFT108J
 FJFT109J

```

FUNCTION TOFT (T, TPRIME, THETA, OMEGA)
  T(T) IS TIME TRANSFORMED TO KIRZAS-LATTER FOR Y
  B=0.359
  FIRST=T-(1.-B*(COS(THETA)**2))*TPRIME
  SECOND=B*(SIN(THETA)**2)*SIN(OMEGA*TPRIME)/OMEGA
  TOFT=FIRST+SECOND
  RETURN 3 END
  
```

C
C
C

FJFT101J
 FJFT102J
 FJFT103J
 FJFT104J
 FJFT105J
 FJFT106J
 FJFT107J
 FJFT108J
 FJFT109J
 FJFT110J
 FJFT111J

```

FUNCTION FOFT(T)
  F(T) IS THE POMRANNING MODEL FOR TIME DEPENDENCE
  OF NUCLEAR REACTIONS YIELD IN RETARDED TIME
  INTEGER OUT
  COMMON OUT, A, B, RV, TD
  TSHAKE=1.E8*T
  DENOM=(B+A*EXP((A+B*(TSHAKE-T)))**RV
  FOFT=(A+B)*EXP(A*(TSHAKE-T))/DENOM
  RETURN 5 END
  
```

C
C
C
C

```

SUBROUTINE ELGFLT(EFLOT,TIME,BIG)
C
C THE FIRST 20 SHAKES OF E(T) IS PLOTTED ON LINEAR SCALES
C
DIMENSION EPLOT(192),TIME(192),E(112),T(112)
MAG = 5 & SMALL = 0.0
CHECK = 0.0
DO 6 I=1,110
E(I)=EFLCT(T) & T(I)=TIME(I)
CONTINUE
CALL PLOT (0.0,-8.0,-3)
CALL PLOT (2.0,2.0,-3)
CALL SCALE (T ,5.,110,1)
CALL SCALE (E ,5.,110,1)
CALL LINE(T ,E ,110,1,0,0)
CALL AXIS(0.,0.,13HTIME (SPAKES),-13,5.,0.,T (111),T (112))
CALL AXIS(0.,0.,12HEFIELD (V/M),12,5.,90.,E (111),E (112))
CALL AXIS(0.,5.,2H ,2,5.,0.,T (111),T (112))
CALL AXIS(5.,0.,2H ,2,5.,90.,E (111),E (112))
CALL FLOT(10.0,2.0,-3)
C
C SMALL VALUES OF E(T) ARE CLIPPED OFF
C AND E(T) IS PLOTTEC ON LCG-LOG SCALES
C
DO 3 I=1,190
IF((EPLCT(I)/BIG).LT.(10.*+(-MAG)))2,3
EFLCT(I)=BIG*(10.*+(-MAG)) & CHECK=1.
CONTINUE
IF(CHECK.EQ.0.) GO TO 11
FRINT 2005
FRINT 2006,(EPLOT(I),I=1,190)
SMALL=EIG*(10.*+(-MAG))
FRINT 2007,SMALL,BIG
CONTINUE
CALL PLOT (0.0,-8.0,-3)
CALL FLOT (2.0,2.0,-3)
EFLT 10
EFLT 20
EFLT 30
EFLT 40
EFLT 50
EFLT 60
EFLT 70
EFLT 80
EFLT 90
EFLT 100
EFLT 110
EFLT 120
EFLT 130
EFLT 140
EFLT 150
EFLT 160
EFLT 170
EFLT 180
EFLT 190
EFLT 200
EFLT 210
EFLT 220
EFLT 230
EFLT 240
EFLT 250
EFLT 260
EFLT 270
EFLT 280
EFLT 290
EFLT 300
EFLT 310
EFLT 320
EFLT 330
EFLT 340
EFLT 350
EFLT 360

```

```

CALL LGSCAL (TIME,5.0,150)
CALL LGSCAL (EPLT,5.0,150)
CALL LGLINE (TIME,EPLT,150,0,0)
CALL LGAXIS (0.,0.,13,TIME (SPAKES),-13,5.,0.,TIME (191),TIME (192))
CALL LGAXIS (0.,0.,12,HEFIELD (V/M),12,5.,90.,EPLT (191),EPLCT (192))
CALL LGAXIS (0.,5.,2H ,2,5.,0.,TIME (191),TIME (192))
CALL LGAXIS (5.,0.,2H ,-2,5.,90.,EPLT (191),EPLT (192))
CALL PLOTE
RETURN
2005 FCRMAT ("1 * * WARNING! PLOT OF E(T) HAS BEEN CLIPPED * * *")
2006 FCRMAT (/5X,"CLIPPED E(T) IS"/19(10(3X,1PE10.3)/))
2007 FCRMAT (/"/ MINIMUM E(T) IS",1PE10.3/" MAXIMUM E(T) IS",1FE10.3EFLT 480
1)
END
EPLT 370
EPLT 380
EPLT 390
EPLT 400
EPLT 410
EPLT 420
EPLT 430
EPLT 440
EPLT 450
EPLT 460
EPLT 470
EPLT 490
EPLT 500

```

Vita

Terry C. Chapman [REDACTED] [REDACTED]

[REDACTED] [REDACTED] He graduated from [REDACTED]

[REDACTED] He attended the University of Colorado in Boulder where he was elected to Tau Beta Pi, Engineering Honor Society and Sigma Pi Sigma, Physics Honor Society. He received the degree Bachelor of Science, Engineering Physics and a commission in the U. S. Air Force from the University of Colorado in 1969. After attending communications training, he was assigned to Kelly AFB, Texas as a communications operations officer in 1970. He entered the Air Force Institute of Technology in 1972.

Permanent Address: [REDACTED] [REDACTED]
[REDACTED] [REDACTED]

This thesis was typed by Ladonna Stitzel.